Naval Research Laboratory
Washington, DC 20375-5320

NRL/MR/6390--12-9380

# Terahertz Spectra of Molecular Clusters of RDX, PETN, and TNT Calculated by Density Functional Theory

L. Huang
S.G. Lambrakos

*Center for Computational Materials Science*
*Materials Science and Technology Division*

A. Shabaev

*George Mason University*
*Fairfax, Virginia*

L. Massa

*Hunter College*
*New York, New York*

March 15, 2012

# REPORT DOCUMENTATION PAGE

*Form Approved*
*OMB No. 0704-0188*



**1. REPORT DATE** *(DD-MM-YYYY)*
15-03-2012

**2. REPORT TYPE**
NRL Memorandum Report

**3. DATES COVERED** *(From - To)*
31-05-2010 – 30-11-2011

**4. TITLE AND SUBTITLE**

Terahertz Spectra of Molecular Clusters of RDX, PETN, and TNT
Calculated by Density Functional Theory

**5a. CONTRACT NUMBER**

**5b. GRANT NUMBER**

**5c. PROGRAM ELEMENT NUMBER**

**6. AUTHOR(S)**

L. Huang, S.G. Lambrakos, A. Shabaev,* and L. Massa†

**5d. PROJECT NUMBER**

**5e. TASK NUMBER**

**5f. WORK UNIT NUMBER**
63-9465-02

**7. PERFORMING ORGANIZATION NAME(S) AND ADDRESS(ES)**

Naval Research Laboratory, Code 6394
4555 Overlook Avenue, SW
Washington, DC 20375-5320

**8. PERFORMING ORGANIZATION REPORT NUMBER**

NRL/MR/6390--12-9380

**9. SPONSORING / MONITORING AGENCY NAME(S) AND ADDRESS(ES)**

Office of Naval Research
One Liberty Center
875 North Randolph Street, Suite 1425
Arlington, VA 22203-1995

**10. SPONSOR / MONITOR'S ACRONYM(S)**

ONR

**11. SPONSOR / MONITOR'S REPORT NUMBER(S)**

**12. DISTRIBUTION / AVAILABILITY STATEMENT**

Approved for public release; distribution is unlimited.

**13. SUPPLEMENTARY NOTES**

*George Mason University, Department of Computation and Data Sciences, Fairfax, VA 22030
†Hunter College, City University of New York, New York, NY 10065

**14. ABSTRACT**

We present calculations of ground state resonance structure associated with molecular clusters of the high explosives RDX, PETN, and TNT using density functional theory (DFT), which is for the construction of parameterized dielectric response functions for excitation by electromagnetic waves at compatible frequencies. These dielectric functions provide for different types of analyses concerning the dielectric response of explosives. In particular, these dielectric response functions provide quantitative initial estimates of spectral response features for subsequent adjustment with respect to additional information such as laboratory measurements and other types of theory based calculations. With respect to qualitative analysis, these spectra provide for the molecular level interpretation of response structure. The DFT software GAUSSIAN was used for the calculations of ground state resonance structure presented here.

**15. SUBJECT TERMS**

Density functional theory (DFT) Explosives
Dielectric functions

| 16. SECURITY CLASSIFICATION OF: | | | 17. LIMITATION OF ABSTRACT | 18. NUMBER OF PAGES | 19a. NAME OF RESPONSIBLE PERSON |
|---|---|---|---|---|---|
| | | | | | Samuel G. Lambrakos |
| **a. REPORT** | **b. ABSTRACT** | **c. THIS PAGE** | UU | 49 | **19b. TELEPHONE NUMBER** *(include area code)* |
| Unclassified | Unclassified | Unclassified | | | (202) 767-2601 |

**Standard Form 298 (Rev. 8-98)**
**Prescribed by ANSI Std. Z39.18**

Contents

## Introduction

A significant aspect of using response spectra calculated by density functional theory, DFT, for the direct construction of dielectric response functions is that it adopts the perspective of computational physics, according to which a numerical simulation represents another source of "experimental" data. This perspective is significant in that a general procedure may be developed for construction of dielectric response functions using DFT calculations as a quantitative initial estimate of spectral response features for subsequent adjustment with respect to additional information such as experimental measurements and other types of theory based calculations. That is to say, for the purpose of simulating many electromagnetic response characteristics of materials, DFT is sufficiently mature for the purpose of generating data complementing, as well as superseding, experimental measurements.

In the case of THz excitation of materials, the procedure of using response spectra calculated using DFT, which is associated with ground state resonance structure, for the direct construction of permittivity functions is well posed owing to the physical characteristic of THz excitation. In particular, it is important to note that the procedure for constructing a permittivity function using response spectra calculated using DFT is physically consistent with the characteristically linear response associated with THz excitation of molecules. Accordingly, one observes a correlation between the advantages of using THz excitation for detection of IEDs (and ambient materials) and those for its numerical simulation based on DFT. Specifically, THz excitation is associated with frequencies that are characteristically perturbative to molecular states, in contrast to frequencies that can induce appreciable electronic state transitions. Of course, the practical aspect of the perturbative character of THz excitation for detection is that detection methodologies can be developed which do not damage materials under examination. The perturbative character of THz excitation with respect to molecular states has significant implications with respect to its numerical simulation based on DFT. It follows then that, owing to the perturbative character of THz excitation, which is characteristically linear, one is able to make a direct association between local oscillations about ground-state minima of a given molecule and THz excitation spectra.

In what follows, calculations are presented of ground state resonance structure associated with molecular clusters of RDX. This resonant structure is for the construction of parameterized dielectric response functions for excitation by electromagnetic waves at compatible frequencies. For this purpose the DFT software GAUSSIAN09 (G09) was adopted [1].

The organization of the subject areas presented here are as follows. First, a general review of the elements of vibrational analysis using DFT that are relevant for the calculation of absorption spectra is presented. Second, a general review is presented concerning the formal structure of permittivity functions in terms of analytic function representations. An understanding of the formal structure of permittivity functions in terms of both physical consistency and causality is important for post-processing of DFT calculations for the purpose of constructing permittivity functions. Third, information concerning the ground state resonance structure of molecular clusters of RDX, PETN and TNT, which are obtained using DFT, is presented as a set of case studies. This information consists of the ground state molecular geometry and response spectra for isolated molecules.

Manuscript approved December 7, 2011.

## Construction of Dielectric Response Functions using DFT

*Density Functional Theory*

The application of density functional theory (DFT) and related methodologies for the determination of electromagnetic response characteristics is important for the analysis of parameter sensitivity. That is to say, many characteristics of the electromagnetic response of a given material may not be detectable, or in general, not relevant for detection. Accordingly, sensitivity analyses concerning the electromagnetic response of layered composite systems can adopt the results of simulations using DFT, and related methodologies, to provide realistic limits on detectability that are independent of a specific system design for IED detection. In addition, analysis of parameter sensitivity based on atomistic response characteristics of a given material, obtained by DFT, provide for an "optimal" best fit of experimental measurements for the construction of permittivity functions. It follows that within the context of parameter sensitivity analysis, data obtained by means of DFT represents a true complement to data that has been obtained by means of experimental measurements.

The DFT software GAUSSIAN09 (G09) can be used to compute an approximation of the IR absorption spectrum of a molecule or molecules [1]. This program calculates vibrational frequencies by determining second derivatives of the energy with respect to the Cartesian nuclear coordinates, and then transforming to mass-weighted coordinates at a stationary point of the geometry. [2]. The IR absorption spectrum is obtained using density functional theory to compute the ground state electronic structure in the Born-Oppenheimer approximation using Kohn-Sham density functional theory [3-7]. GAUSSIAN uses specified orbital basis functions to describe the electronic wavefunctions and density. For a given set of nuclear positions, the calculation directly gives the electronic charge density of the molecule, the potential energy *V*, and the displacements in Cartesian coordinates of each atom. The procedure for vibrational analysis followed in GAUSSIAN is that described in [8]. Reference [9] presents a fairly detailed review of this procedure. A brief description of this procedure is as follows.

The procedure followed by GAUSSIAN is based on the fact the vibrational spectrum depends on the Hessian matrix $\mathbf{f}_{\text{CART,}}$ which is constructed using the second partial derivatives of the potential energy *V* with respect to displacements of the atoms in Cartesian coordinates. Accordingly, the elements of the *3N* x *3N* matrix $\mathbf{f}_{\text{CART}}$ are given by

$$f_{\text{CART}ij} = \left(\frac{\partial^2 V}{\partial \xi_i \partial \xi_j}\right)_0 \qquad (1)$$

where $\{\xi_1,\xi_2,\xi_3,\xi_4,\xi_5,\xi_6,...,\xi_{3N}\} = \{\Delta x_1,\Delta y_1,\Delta z_1,\Delta x_2,\Delta y_2,\Delta z_2,...,\Delta z_N\}$, which are displacements in Cartesian coordinates, and *N* is the number of atoms. As discussed above, the zero subscript in Eq.(1) indicates that the derivatives are taken at the equilibrium positions of the atoms, and that the first derivatives are zero. Given the Hessian matrix defined by Eq.(1) the operations for calculation of the vibrational spectrum require that the Hessian matrix Eq.(1) be transformed to mass-weighted Cartesian coordinates according to the relation

$$f_{\text{MWC}ij} = \frac{f_{\text{CART}ij}}{\sqrt{m_i m_j}} = \left(\frac{\partial^2 V}{\partial q_i \partial q_j}\right)_0 \qquad (2)$$

where $\{q_1,q_2,q_3,q_4,q_5,q_6,...,q_{3N}\} = \{\sqrt{m_1}\Delta x_1,\sqrt{m_1}\Delta y_1,\sqrt{m_1}\Delta z_1,\sqrt{m_2}\Delta x_2,\sqrt{m_2}\Delta y_2,\sqrt{m_2}\Delta z_2,...,\sqrt{m_N}\Delta z_N\}$ are the mass-weighted Cartesian coordianates. GAUSSIAN computes the energy second derivatives Eq.(2), thus computing the forces for displacement perturbations of each atom along each Cartesian direction. The first derivatives of the dipole moment with respect to atomic positions $\partial\bar{\mu}/\partial\xi_i$ are also computed. Each vibrational eigenmode leads to one peak in the absorption spectrum, at a frequency equal to the mode's eigenfrequency $\nu_{n0}$. The absorption intensity corresponding to a particular eigenmode *n* whose eigenfrequency is $\nu_{n0}$ is given by

$$I_n = \frac{\pi}{3c}\left|\sum_{i=1}^{3N}\frac{\partial\vec{\mu}}{\partial\xi_i}l_{\mathrm{CART}in}\right|^2, \tag{3}$$

where $\mathbf{l}_{\mathrm{CART}}$ is the matrix whose elements are the displacements of the atoms in Cartesian coordinates. The matrix $\mathbf{l}_{\mathrm{CART}}$ is determined by the following procedure. First,

$$\mathbf{l}_{\mathrm{CART}} = \mathbf{M}\mathbf{l}_{\mathrm{MWC}}\ , \tag{4}$$

where $\mathbf{l}_{\mathrm{MWC}}$ is the matrix whose elements are the displacements of the atoms in mass-weighted Cartesian coordinates and **M** is a diagonal matrix defined by the elements

$$M_{ii} = \frac{1}{\sqrt{m_i}}\ . \tag{5}$$

Proceeding, $\mathbf{l}_{\mathrm{MWC}}$ is the matrix needed to diagonalize $\mathbf{f}_{\mathrm{MWC}}$ defined by Eq.(2) such that

$$(\mathbf{l}_{\mathrm{MWC}})^{\mathrm{T}}\,\mathbf{f}_{\mathrm{MWC}}(\mathbf{l}_{\mathrm{MWC}}) = \Lambda\ , \tag{6}$$

where $\Lambda$ is the diagonal matrix with eigenvalues $\lambda_i$. The procedure for diagonalizing Eq.(6) consists of the operations

$$\mathbf{f}_{\mathrm{INT}} = (\mathbf{D})^{\mathrm{T}}\,\mathbf{f}_{\mathrm{MWC}}(\mathbf{D}) \tag{7}$$

and

$$(\mathbf{L})^{\mathrm{T}}\,\mathbf{f}_{\mathrm{MWC}}(\mathbf{L}) = \Lambda\ , \tag{8}$$

where **D** is a matrix transformation to coordinates where rotation and translation have been separated out and **L** is the transformation matrix composed of eigenvectors calculated according to Eq.(8). The eigenfrequencies in units of ($cm^{-1}$) are calculated using the eigenvalues $\lambda_n$ by the expression

$$\nu_{n0} = \frac{\sqrt{\lambda_n}}{2\pi c}\ , \tag{9}$$

where *c* is the speed of light. The elements of $\mathbf{l}_{\mathrm{CART}}$ are given by

$$l_{\mathrm{CART}ki} = \sum_{j=1}^{3N}\frac{D_{kj}L_{ji}}{\sqrt{m_j}}\ , \tag{10}$$

where *k, i=1,…, 3N,* and the column vectors of these elements are the normal modes in Cartesian coordinates.

The intensity Eq.(3) must then be multiplied by the number density of molecules to give an absorption strength. It follows that the absorption spectrum calculated by GAUSSIAN is a sum of delta functions whose positions and magnitudes correspond to the vibrational frequencies and magnitudes, respectively. In principle, however, these spectral components must be broadened and shifted to account for anharmonic effects such as finite mode lifetimes and inter-mode couplings.

*Dielectric Response Functions*

The general approach of constructing permittivity functions according to the best fit of available data for given material corresponding to many different types of experimental measurements has been typically the dominant approach. The present study extends this approach in that calculations of electromagnetic response based on DFT are also adopted as data for construction of permittivity functions. The inclusion of this type of information is significant for accessing what spectral response features at the molecular level are actually detectable with respect to a given set of detection parameters. Accordingly, permittivity functions having been constructed using DFT calculations provide a quantitative correlation between macroscopic material response and molecular structure. Within this context it is not important that the permittivity function be quantitatively accurate for the purpose of being adopted as input for system simulation. Rather, it is important that the permittivity function be qualitatively accurate in terms of specific dielectric response features for the purpose of sensitivity analysis, which is relevant for the assessment of absolute detectability of different types of molecular structure with respect to a given set of detection parameters. That is to say, permittivity functions that have been determined using DFT can provide a mechanistic interpretation of material response to electromagnetic excitation that could establish the well posedness of a given detection methodology for detection of specific molecular characteristics. Within the context of practical application, permittivity functions having been constructed according to the best fit of available data would be "correlated" with those obtained using DFT for proper interpretation of permittivity-function features. Subsequent to establishment of good correlation between DFT and experiment, DFT calculations can be adopted as constraints for the purpose of constructing permittivity functions, whose features are consistent with molecular level response, for adjustment relative to specific sets of either experimental data or additional molecular level information.

The construction of permittivity functions using DFT calculations involves, however, an aspect that requires serious consideration. This aspect concerns the fact that a specific parametric function representation must be adopted. Accordingly, any parametric representation, i.e., parameterization, adopted for permittivity-function construction must be physically consistent with specific molecular response characteristics, while limiting the inclusion of feature characteristics that tend to mask response signatures that may be potentially detectable.

In principle, parameterizations are of two classes. One class consists of parameterizations that are directly related to molecular response characteristics. This class of parameterizations would include spectral scaling and width coefficients. The other class consists of parameterizations that are purely phenomenological and are structured for optimal and convenient best fits to experimental measurements. A sufficiently general parameterization of permittivity functions is given by Drude-Lorentz approximation [10]

$$\varepsilon(\nu) = \varepsilon'(\nu) + i\varepsilon''(\nu) = \varepsilon_\infty + \sum_{n=1}^{N} \frac{\nu_{np}^2}{(\nu_{no}^2 - \nu^2) - i\gamma_n \nu} \ , \tag{11}$$

where $\nu_{np}$ and $\gamma_n$ are the spectral scaling and width of a resonance contributing to the permittivity function. The permittivity $\varepsilon_\infty$ is a constant since the dielectric response at high frequencies is substantially detuned from the probe frequency. The real and imaginary parts, $\varepsilon_r(\nu)$ and $\varepsilon_i(\nu)$, respectively, of the permittivity function can be written separately as

$$\varepsilon_r(\nu) = \varepsilon_\infty + \sum_{n=1}^{N} \frac{\nu_{np}^2(\nu_{no}^2 - \nu^2)}{(\nu_{no}^2 - \nu^2)^2 + \gamma_n^2\nu^2} \quad \text{and} \quad \varepsilon_i(\nu) = \sum_{n=1}^{N} \frac{\nu_{np}^2 \gamma_n \nu}{(\nu_{no}^2 - \nu^2)^2 + \gamma_n^2\nu^2} \ . \tag{12}$$

With respect to practical application, the absorption coefficient $\alpha$ and index of refraction $n_r$, given by

$$\alpha = \frac{4\pi\nu}{\sqrt{2}}\left[-\varepsilon_r + \sqrt{\varepsilon_r^2 + \varepsilon_i^2}\right]^{1/2} \quad \text{and} \quad n_r = \frac{1}{\sqrt{2}}\left[\varepsilon_r + \sqrt{\varepsilon_r^2 + \varepsilon_i^2}\right]^{1/2}, \tag{13}$$

respectively, provide direct relationships between calculated quantities obtained by DFT and the "conveniently measurable" quantities $\alpha$ and $n_r$. It is significant to note that in what follows, the absorption coefficient $\alpha$ is determined using DFT calculated spectra in the same spirit as for its measurement in the laboratory. Although permittivity functions $\varepsilon(\nu)$ are not determined explicitly in the present study, it must be kept in mind that the ultimate construction of these functions is necessary for using DFT calculated spectra to model the dielectric response of complex composite materials and associated detector designs [11].

## Ground State Resonance Structure of Molecular Clusters of RDX

In this section are presented the results of computational experiments using DFT concerning molecular clusters of RDX. These results include the relaxed or equilibrium configuration of a single isolated molecule of RDX (see Table 1) and ground-state oscillation frequencies and IR intensities for this configuration, which are calculated by DFT according to the frozen phonon approximation (see Table 2). The ground state resonance structure for a single isolated molecule of RDX is adopted as a reference for analysis of spectral features associated with molecular clusters of different sizes. For these calculations geometry optimization and vibrational analysis was effected using the DFT model B3LYP [12, 13] and basis function 6-311G(2d,2p) [14,15]. According to the specification of this basis function, (2d,2p) designates polarization functions having 2 sets of d functions for heavy atoms and 2 sets of p functions for hydrogen atoms [16]. A schematic representation of the molecular geometry of a single isolated molecule of RDX is shown in Fig.(1). A schematic representation of molecular geometries of molecular clusters consisting of 2, 4 and 6 molecules are shown in Figs. (2), (3) and (4), respectively. It is significant to note that the relative positions of the molecules associated with each of the molecular clusters is according to crystallographic structure conditions that would be associated with bulk material. In particular, the crystal structure of $\alpha-$RDX, whose CCDC reference code is CTMTNA, has been investigated by C. S. Choi and E. Prince [17]. The space group for this crystal structure is ***Pbca*** (symmetry operators are x, y, z; 1/2-x, -y, 1/2+z; 1/2+x, 1/2-y, -z; -x, 1/2+y, 1/2-z; -x, -y, -z; 1/2+x, y, 1/2-z; 1/2-x, 1/2+y, z; x, 1/2-y, 1/2+z), and the unit cell constants are a=13.182, b=11.574, c=10.709, $\alpha$=0.00, $\beta$=90.00, $\gamma$=90.00 and density 1.806 g/cm$^3$. The ground-state oscillation frequencies and IR intensities for the different molecular clusters of RDX, corresponding to their relaxed equilibrium configurations, are calculated by DFT according to the frozen phonon approximation. In the cases of molecular clusters of 2, 4 and 6 molecules, these values are given in Tables 3, 4 and 5, respectively. The DFT model and basis function used for these calculations are the same as those used for the single isolated molecule of RDX. Two programs, ConQuest and Mercury [18], have been used for searching the Cambridge Structural Database (CSD), visualizing database entries, RDX, and creating the n-molecule clusters. We have considered the interactions and forces between the single molecule and its neighborhood when we created the cluster. Hydrogen bonding between the molecules is important for establishing the cluster.

The DFT calculated absorption spectra given in tables 3, 4 and 5 provide information for analysis of dielectric response with respect to the size of molecular clusters, i.e., the denumeration of ground state resonance modes and estimates of molecular level dielectric response structure. The construction of permittivity functions using the DFT calculated absorption spectra follows the same procedure as that applied for the construction of permittivity functions using experimentally measured absorption spectra, but with the addition of certain constraint conditions. Accordingly, construction of permittivity functions using either DFT or experimentally measured absorption spectra requires parameterizations that are in terms of physically consistent analytic function representations such as the Drude-Lorentz model, i.e., Eqs.(11) and (12). Although the formal structure of permittivity functions constructed using DFT and experimental measurements are the same, their interpretation with respect to parameterization is different for each case.

**Table 1.** Atomic positions of RDX (Å) after geometry optimization.

| Atomic number | X | Y | Z | Atomic number | X | Y | Z |
|---|---|---|---|---|---|---|---|
| 7 | 1.177132 | -0.800831 | 0.102459 | 8 | -1.148702 | 1.861918 | 2.523892 |
| 7 | 0.102459 | 1.177132 | -0.800831 | 8 | 3.333613 | -0.184585 | 0.086238 |
| 7 | -0.800831 | 0.102459 | 1.177132 | 8 | 0.086238 | 3.333613 | -0.184585 |
| 7 | 2.436639 | -0.679768 | 0.742611 | 8 | -0.184585 | 0.086238 | 3.333613 |
| 7 | 0.742611 | 2.436639 | -0.679768 | 1 | -1.515435 | 1.871323 | 0.32473 |
| 7 | -0.679768 | 0.742611 | 2.436639 | 1 | 0.32473 | -1.515435 | 1.871323 |
| 6 | -1.083455 | 0.93108 | 0.011066 | 1 | 1.871323 | 0.32473 | -1.515435 |
| 6 | 0.011066 | -1.083455 | 0.93108 | 1 | -1.794386 | 0.385919 | -0.609699 |
| 6 | 0.93108 | 0.011066 | -1.083455 | 1 | -0.609699 | -1.794386 | 0.385919 |
| 8 | 2.523892 | -1.148702 | 1.861918 | 1 | 0.385919 | -0.609699 | -1.794386 |
| 8 | 1.861918 | 2.523892 | -1.148702 | | | | |

Before proceeding with further discussion concerning various features of dielectric response with respect to the size of molecular clusters, it is necessary to again indicate two general goals underlying the DFT calculations presented here and in related studies. These goals are, first, to obtain an understanding of the physical nature underlying the various spectral features associated with the dielectric response of materials, and second, the construction of dielectric response functions for use in quantitative simulation of detector designs and their associated detection scenarios. With respect to the second goal, the DFT calculated absorption spectra given above are to be considered the results of computational experiments for the purpose of being correlated, as well as combined, with other absorption spectra, which may be the results of both computational experiments and laboratory measurements. Accordingly, the dielectric response of a molecular cluster consisting of a given number of molecules can be associated with response features that are intermediate between that of isolated molecules and that of the bulk lattice response. It follows that for analysis of spectra, permittivity functions for finite size molecular clusters can be adopted for use in effective medium theories in order to model the dielectric response of composite materials. This follows in that a composite material may be characterized by a non-interacting uniform distribution of finite-size molecular clusters within a host material. Models based on this type of characterization are for further investigation.

Proceeding, shown in Figs. 6, 7, 8 and 9 are calculated IR intensities for a single isolated molecule, 2-molecule cluster, 4-molecule cluster and 6-molecule cluster, respectively. Referring to Figs. 10 and 11, one notes continuous spectra consisting of a superposition of essentially Lorenzian functions of various heights and widths, which have been constructed using discrete spectra. Although the primarily purpose of this type of construction within GAUSSIAN is for the purpose of enhanced visualization of spectral features, it is significant to note that this operation represents an estimation of the characteristic scaling and width of resonances contributing the dielectric response. With respect to the interrelationship between the absorption coefficient $\alpha$ and the permittivity function $\varepsilon(\nu)$ defined by Eqs.(11), (12) and (13), this represents an estimation of the parameters $\nu_{np}$ and $\gamma_n$, which are the spectral scaling and width of a resonance contributing to the permittivity function. For qualitative comparison of spectral features this type of estimate should be sufficient. For the construction of permittivity functions using DFT calculated spectra for subsequent use for quantitative simulation, it is more appropriate, however, to assume the parameters $\nu_{np}$ and $\gamma_n$ adjustable, i.e., to be assigned values according to additional information.

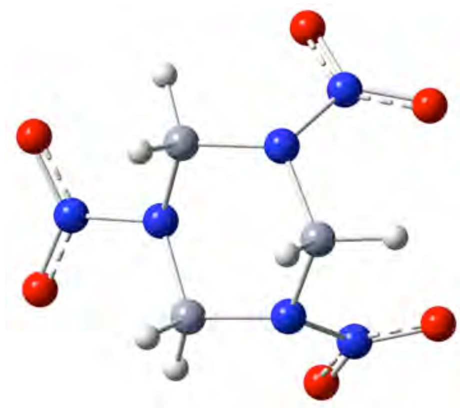

**Figure 1.** Molecular Geometry of RDX.

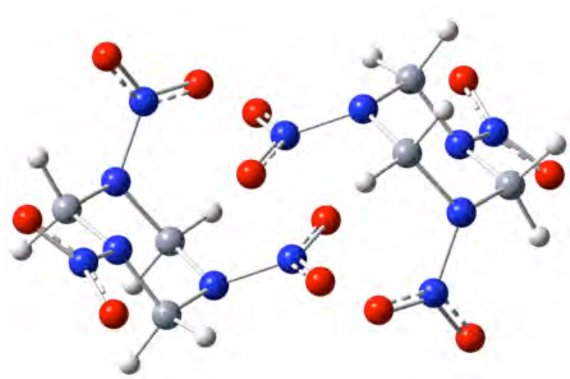

**Figure 2.** Molecular Geometry of 2-Molecule Cluster of RDX.

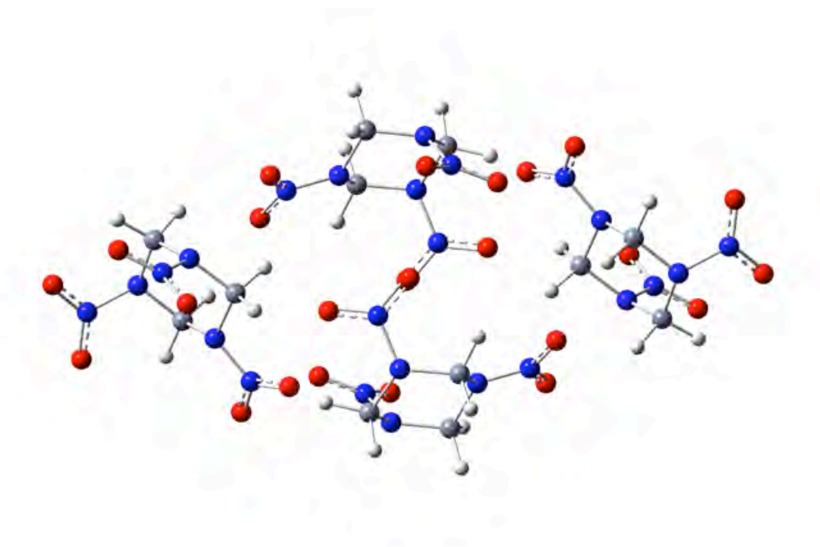

**Figure 3.** Molecular Geometry of 4-Molecule Cluster of RDX.

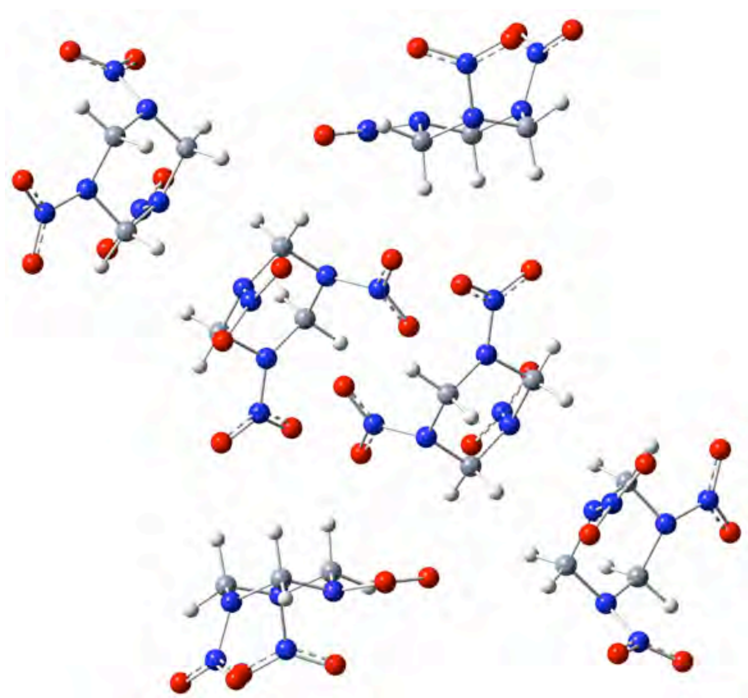

**Figure 4.** Molecular Geometry of 6-Molecule Cluster of RDX.

**Table 2.** Oscillation frequencies and IR intensities for single isolated molecule of RDX.

| Frequency $cm^{-1}$ | Intensity (km/mol) | Frequency $cm^{-1}$ | Intensity (km/mol) | Frequency $cm^{-1}$ | Intensity (km/mol) | Frequency $cm^{-1}$ | Intensity (km/mol) |
|---|---|---|---|---|---|---|---|
| 42.2254 | 0.0182 | 584.6074 | 10.0692 | 1024.3428 | 168.8792 | 1467.5898 | 39.3506 |
| 56.9758 | 2.521 | 592.499 | 0.9828 | 1044.7485 | 37.0924 | 1482.6062 | 2.6857 |
| 61.6615 | 1.2995 | 613.8533 | 15.7407 | 1161.983 | 1.5664 | 1499.7183 | 46.3106 |
| 74.6522 | 0.0198 | 656.5469 | 0.0877 | 1237.517 | 20.8868 | 1663.0582 | 150.5 |
| 93.4908 | 0.1868 | 681.3616 | 4.103 | 1247.1127 | 39.6523 | 1683.8234 | 223.9439 |
| 114.9468 | 0.0237 | 764.6259 | 1.6194 | 1270.7874 | 6.6058 | 1701.8562 | 377.1413 |
| 210.9971 | 7.4608 | 773.8667 | 0.4212 | 1270.868 | 70.4238 | 3016.3838 | 4.5269 |
| 222.2105 | 1.3202 | 783.2278 | 2.4613 | 1310.4281 | 336.5103 | 3018.0322 | 39.0865 |
| 290.7538 | 0.001 | 808.6349 | 61.0009 | 1311.0815 | 125.0556 | 3082.2839 | 15.4483 |
| 327.5155 | 2.1052 | 860.6995 | 34.5479 | 1346.6562 | 61.2854 | 3216.2893 | 12.8591 |
| 378.0279 | 0.0344 | 874.637 | 5.7883 | 1361.4716 | 4.2675 | 3221.1511 | 12.1171 |
| 410.0315 | 0.3607 | 902.7032 | 38.0133 | 1370.1674 | 132.9406 | 3222.6191 | 7.9466 |
| 413.9516 | 9.1916 | 922.3189 | 232.1041 | 1376.7496 | 6.1702 | | |
| 439.9936 | 9.9427 | 947.0868 | 178.6166 | 1410.854 | 11.1317 | | |
| 472.7935 | 15.7833 | 961.2388 | 110.5947 | 1425.8851 | 95.0582 | | |

**Table 3.** Oscillation frequencies and IR intensities for 2-molecule cluster of RDX.

| Frequency $cm^{-1}$ | Intensity (km/mol) | Frequency $cm^{-1}$ | Intensity (km/mol) | Frequency $cm^{-1}$ | Intensity (km/mol) | Frequency $cm^{-1}$ | Intensity (km/mol) |
|---|---|---|---|---|---|---|---|
| 14.9682 | 0.2645 | 410.6108 | 18.9557 | 928.1564 | 0 | 1380.856 | 0 |
| 26.1434 | 2.6138 | 411.9108 | 0 | 933.6769 | 388.6451 | 1380.9839 | 14.262 |
| 29.3972 | 0 | 431.3649 | 26.9949 | 947.9423 | 0 | 1413.2908 | 0 |
| 35.0656 | 1.686 | 431.9862 | 0 | 951.4927 | 389.1337 | 1413.4794 | 26.0848 |
| 48.6587 | 0 | 462.2036 | 0 | 965.8482 | 0 | 1426.1849 | 170.412 |
| 48.8051 | 0.8348 | 462.2959 | 24.2307 | 967.4657 | 120.6746 | 1426.6543 | 0 |
| 52.4387 | 0 | 588.422 | 20.4808 | 1032.6176 | 0 | 1467.2236 | 97.7646 |
| 58.4871 | 6.7772 | 588.5022 | 0 | 1033.149 | 340.5911 | 1467.9124 | 0 |
| 60.7165 | 0 | 602.5717 | 0 | 1047.2354 | 0 | 1485.0341 | 7.5186 |
| 69.1863 | 0 | 602.7465 | 4.1501 | 1048.9814 | 84.5362 | 1485.3751 | 0 |
| 86.8182 | 2.2742 | 615.5301 | 0 | 1169.7606 | 0 | 1501.0522 | 94.1043 |
| 90.5851 | 0 | 615.8413 | 33.0986 | 1169.8094 | 1.5371 | 1501.2987 | 0 |
| 91.258 | 0.4119 | 661.6494 | 0.6713 | 1246.179 | 0 | 1657.328 | 179.9943 |
| 96.1505 | 0 | 661.679 | 0 | 1246.2902 | 38.9162 | 1658.2531 | 0 |
| 100.3821 | 0.172 | 685.3188 | 0 | 1257.6866 | 0 | 1662.3564 | 0 |
| 113.2955 | 0 | 686.3688 | 5.5564 | 1258.2448 | 66.1412 | 1677.2478 | 601.3396 |
| 124.3702 | 0.4582 | 766.0924 | 16.4961 | 1266.9543 | 23.0611 | 1695.8433 | 0 |
| 134.6481 | 0 | 766.169 | 0 | 1266.9575 | 0 | 1696.4061 | 565.5932 |
| 212.6795 | 13.8607 | 770.9064 | 1.8229 | 1272.184 | 0 | 3009.2444 | 38.2081 |
| 213.2402 | 0 | 773.5341 | 0 | 1272.4142 | 135.649 | 3009.2595 | 0 |
| 215.3385 | 0 | 778.6134 | 0 | 1306.4919 | 564.6394 | 3013.1033 | 77.6467 |
| 221.1027 | 2.4114 | 779.4847 | 10.866 | 1307.7988 | 0 | 3013.2798 | 0 |
| 293.015 | 0 | 803.2578 | 164.0284 | 1310.0482 | 0 | 3076.2737 | 38.0099 |
| 293.6024 | 0.0206 | 806.1595 | 0 | 1312.1539 | 294.3002 | 3076.3501 | 0 |
| 327.11 | 7.3232 | 862.963 | 74.0208 | 1348.7789 | 0 | 3215.1035 | 0 |
| 327.3015 | 0 | 864.6105 | 0 | 1350.2686 | 101.1641 | 3215.1763 | 23.6244 |
| 374.0134 | 0 | 876.7775 | 0 | 1363.9604 | 0 | 3218.981 | 0 |
| 374.1297 | 0.0955 | 877.259 | 4.6032 | 1364.0728 | 7.9788 | 3219.0559 | 28.491 |
| 406.1292 | 0 | 901.3114 | 68.6632 | 1370.1343 | 0 | 3220.7827 | 17.6924 |
| 406.6222 | 2.8765 | 901.419 | 0 | 1374.3319 | 331.9773 | 3220.7993 | 0 |

**Table 4.** Oscillation frequencies and IR intensities for 4-molecule cluster of RDX.

| Frequency $cm^{-1}$ | Intensity (km/mol) | Frequency $cm^{-1}$ | Intensity (km/mol) | Frequency $cm^{-1}$ | Intensity (km/mol) | Frequency $cm^{-1}$ | Intensity (km/mol) |
|---|---|---|---|---|---|---|---|
| 5.9417 | 0.8932 | 218.3001 | 0 | 681.218 | 5.0704 | 1049.8677 | 216.8569 |
| 11.2558 | 0 | 227.3244 | 3.589 | 681.2275 | 0 | 1050.019 | 0 |
| 12.1643 | 1.8844 | 227.3429 | 0 | 685.1279 | 0 | 1050.8359 | 183.4953 |
| 17.1016 | 0.7561 | 292.3184 | 0 | 686.3152 | 2.8861 | 1057.8466 | 0 |
| 18.0733 | 0 | 292.3708 | 0.0697 | 763.4879 | 2.4633 | 1059.7562 | 409.959 |
| 22.1499 | 0.8163 | 297.7226 | 0 | 763.5641 | 0 | 1152.1003 | 0 |
| 28.6989 | 0 | 298.443 | 0.5903 | 765.5928 | 0 | 1152.1033 | 3.507 |
| 30.4139 | 3.2113 | 334.8958 | 0 | 765.6132 | 3.4463 | 1165.8265 | 0 |
| 30.6346 | 0 | 334.9269 | 6.8163 | 769.1978 | 7.4405 | 1165.8674 | 2.651 |
| 32.9922 | 5.0297 | 336.7472 | 5.1234 | 771.9295 | 0 | 1241.8436 | 129.8683 |
| 34.6379 | 2.1739 | 336.9161 | 0 | 775.0354 | 0 | 1242.0962 | 0 |
| 37.3103 | 0 | 373.1536 | 0 | 775.0493 | 24.4915 | 1243.5063 | 0 |
| 43.0674 | 0 | 373.2618 | 0.3094 | 775.3522 | 0 | 1243.582 | 64.6015 |
| 46.2171 | 0.254 | 382.1399 | 0.0763 | 775.3527 | 0.5402 | 1250.0132 | 0 |
| 48.6162 | 0 | 382.1516 | 0 | 785.7931 | 0 | 1250.8424 | 130.1652 |
| 53.1727 | 0 | 404.5152 | 38.1485 | 785.8521 | 23.2646 | 1260.1033 | 0 |
| 53.5529 | 1.984 | 405.4077 | 0 | 799.5599 | 113.6132 | 1260.714 | 52.2322 |
| 55.7237 | 0.3531 | 409.244 | 0 | 801.5757 | 0 | 1267.402 | 28.1434 |
| 56.7595 | 0 | 409.8144 | 0.4239 | 807.4271 | 177.408 | 1267.7118 | 0 |
| 59.5683 | 0 | 411.4004 | 2.0287 | 807.6755 | 0 | 1270.1116 | 0 |
| 63.8558 | 2.6444 | 411.5578 | 0 | 853.126 | 0 | 1271.1813 | 226.9784 |
| 64.0555 | 0 | 415.4892 | 26.128 | 853.1605 | 70.288 | 1274.3192 | 109.6892 |
| 64.2175 | 2.9595 | 415.5214 | 0 | 857.0704 | 37.5648 | 1274.6527 | 0 |
| 68.6191 | 0 | 428.8975 | 22.651 | 857.843 | 0 | 1279.0389 | 0 |
| 72.4516 | 8.4016 | 429.463 | 0 | 874.676 | 0 | 1279.0677 | 13.0795 |
| 75.5401 | 0 | 452.5779 | 59.8655 | 875.0377 | 19.4847 | 1305.5767 | 304.1009 |
| 79.1997 | 1.2599 | 452.8454 | 0 | 875.1404 | 3.0135 | 1308.7438 | 0 |
| 80.1933 | 0 | 468.1582 | 0 | 875.1481 | 0 | 1311.9091 | 0 |
| 83.536 | 7.8691 | 468.3085 | 13.3874 | 895.7402 | 78.105 | 1312.7611 | 288.9891 |
| 90.1537 | 0 | 482.5359 | 74.0979 | 897.0327 | 0 | 1313.2223 | 0 |
| 93.6963 | 6.4259 | 482.6726 | 0 | 903.7427 | 29.171 | 1314.9039 | 986.756 |
| 102.0439 | 1.0454 | 589.0296 | 0 | 903.7535 | 0 | 1318.5479 | 0 |
| 102.3205 | 0 | 589.1119 | 20.029 | 925.3393 | 250.4504 | 1320.8827 | 487.5419 |
| 114.0193 | 0 | 592.5375 | 1.1143 | 925.3761 | 0 | 1348.9429 | 0 |
| 119.1062 | 0.1219 | 592.5639 | 0 | 925.9388 | 0 | 1350.5767 | 152.6872 |
| 120.8635 | 0 | 596.34 | 29.464 | 930.7203 | 475.2726 | 1353.9634 | 0 |
| 120.9227 | 0.0928 | 596.5048 | 0 | 943.2045 | 0 | 1354.9141 | 175.168 |
| 124.0232 | 0.3339 | 604.0503 | 0 | 945.0859 | 397.0026 | 1367.0991 | 0 |
| 124.0666 | 0 | 604.199 | 0.7334 | 954.5926 | 468.9313 | 1367.1254 | 22.7386 |
| 128.5985 | 0 | 614.1897 | 0 | 955.4067 | 0 | 1368.368 | 0 |
| 145.2666 | 0 | 615.0315 | 78.044 | 968.2669 | 0 | 1368.5292 | 1.3385 |
| 147.8037 | 1.5142 | 619.4185 | 0 | 970.01 | 145.2878 | 1377.3337 | 0 |
| 187.6243 | 0 | 619.5198 | 45.152 | 970.8496 | 0 | 1378.8676 | 210.1102 |
| 193.0925 | 1.2304 | 657.7129 | 0.3953 | 972.0773 | 116.258 | 1383.1447 | 0 |
| 212.9453 | 9.0403 | 657.7307 | 0 | 1048.3354 | 0 | 1384.4601 | 128.5912 |
| 212.9988 | 0 | 658.9496 | 5.8763 | 1048.5754 | 113.7712 | 1387.149 | 0 |
| 217.5362 | 17.2925 | 659.1081 | 0 | 1048.6093 | 0 | 1387.1785 | 19.1128 |

**Table 4.** (continued)

| Frequency $cm^{-1}$ | Intensity (km/mol) | Frequency $cm^{-1}$ | Intensity (km/mol) | Frequency $cm^{-1}$ | Intensity (km/mol) | Frequency $cm^{-1}$ | Intensity (km/mol) |
|---|---|---|---|---|---|---|---|
| 1388.3368 | 0 | 1482.5695 | 0 | 1696.0105 | 0 | 3109.188 | 6.2155 |
| 1389.1818 | 197.8481 | 1486.8042 | 0 | 1696.0919 | 958.9728 | 3216.2964 | 0 |
| 1418.2656 | 0 | 1486.9224 | 6.0855 | 1697.5343 | 0 | 3216.3967 | 23.3328 |
| 1418.4442 | 69.7893 | 1497.5839 | 99.1629 | 1698.3257 | 435.5343 | 3218.6729 | 0 |
| 1419.0931 | 0 | 1497.9727 | 0 | 3028.8118 | 34.3859 | 3218.7385 | 66.0843 |
| 1419.1238 | 20.7794 | 1506.0269 | 71.3172 | 3028.8286 | 0 | 3221.2642 | 0 |
| 1427.403 | 0 | 1506.0958 | 0 | 3033.7673 | 45.2205 | 3221.2849 | 71.082 |
| 1429.0955 | 182.339 | 1614.6718 | 172.3449 | 3033.8721 | 0 | 3223.749 | 32.0502 |
| 1433.496 | 329.1365 | 1618.0834 | 0 | 3057.082 | 0 | 3223.7571 | 0 |
| 1434.8369 | 0 | 1622.3704 | 0 | 3057.0933 | 2.066 | 3225.3008 | 25.2271 |
| 1456.7389 | 112.6976 | 1624.3489 | 520.7316 | 3062.8665 | 11.5487 | 3225.3062 | 0 |
| 1457.354 | 0 | 1640.2415 | 0 | 3062.8721 | 0 | 3228.2629 | 28.9712 |
| 1475.7458 | 0 | 1652.6211 | 494.1416 | 3095.7844 | 13.1672 | 3228.2712 | 0 |
| 1475.816 | 45.857 | 1675.8097 | 0 | 3095.8081 | 0 | | |
| 1482.1519 | 14.8717 | 1675.9667 | 267.4778 | 3109.1875 | 0 | | |

**Table 5.** Oscillation frequencies and IR intensities for 6-molecule cluster of RDX.

| Frequency $cm^{-1}$ | Intensity (km/mol) | Frequency $cm^{-1}$ | Intensity (km/mol) | Frequency $cm^{-1}$ | Intensity (km/mol) | Frequency $cm^{-1}$ | Intensity (km/mol) |
|---|---|---|---|---|---|---|---|
| 4.3759 | 0.052 | 81.9255 | 0 | 382.4558 | 0 | 657.5724 | 0.0572 |
| 6.3809 | 0.4456 | 86.685 | 8.0455 | 382.4635 | 0.184 | 663.3732 | 0 |
| 6.6603 | 0 | 90.8211 | 0 | 396.9643 | 14.1359 | 663.6753 | 4.3512 |
| 8.3081 | 1.5655 | 92.2727 | 12.5623 | 397.1129 | 0 | 680.6752 | 0 |
| 11.3305 | 1.1677 | 94.7594 | 0.7639 | 401.1577 | 6.1866 | 680.6866 | 4.1544 |
| 11.4291 | 0 | 94.7711 | 0 | 401.2039 | 0 | 686.9826 | 0 |
| 13.5796 | 0 | 100.6031 | 0 | 406.1711 | 0 | 687.2872 | 0.3263 |
| 15.5115 | 0 | 101.9998 | 1.2895 | 406.3565 | 19.1602 | 690.2896 | 0 |
| 18.5873 | 1.6704 | 114.5513 | 0 | 409.9726 | 1.8507 | 690.3004 | 9.8633 |
| 20.9307 | 3.5563 | 118.8257 | 0.393 | 410.033 | 0 | 764.5281 | 28.3151 |
| 21.1463 | 0 | 119.7657 | 0 | 413.1681 | 0 | 764.6277 | 0 |
| 21.7823 | 1.194 | 121.2679 | 0 | 413.1752 | 19.0126 | 765.3242 | 2.2033 |
| 24.7982 | 0 | 121.3376 | 0.0639 | 414.8473 | 28.0452 | 765.3998 | 0 |
| 25.0879 | 1.4846 | 122.214 | 0.4227 | 414.9183 | 0 | 766.1323 | 10.3475 |
| 28.8329 | 0 | 125.993 | 0 | 431.0954 | 19.0787 | 766.535 | 0 |
| 29.6123 | 2.1614 | 131.7202 | 2.9282 | 431.6634 | 0 | 767.5119 | 6.1219 |
| 31.0821 | 2.4051 | 131.7806 | 0 | 439.8429 | 0 | 768.0571 | 0 |
| 31.4382 | 0 | 136.3106 | 0 | 439.8558 | 15.3285 | 770.9393 | 9.0595 |
| 33.4071 | 0 | 138.8273 | 0.5152 | 451.8383 | 61.9663 | 771.0958 | 0 |
| 34.9247 | 4.8311 | 187.4796 | 0 | 452.0278 | 0 | 774.2007 | 33.164 |
| 34.9452 | 0 | 191.0382 | 1.5234 | 471.8306 | 0 | 774.2167 | 0 |
| 43.3381 | 0.5939 | 209.4877 | 17.7486 | 472.242 | 15.1678 | 774.9939 | 0 |
| 43.4133 | 0 | 209.5666 | 0 | 475.251 | 24.5623 | 774.9948 | 0.4784 |
| 44.9009 | 0 | 212.7895 | 9.2759 | 475.2595 | 0 | 782.3235 | 0 |
| 48.2995 | 0.1558 | 212.8572 | 0 | 482.1034 | 75.0025 | 782.3255 | 7.2197 |
| 49.2102 | 3.4005 | 216.833 | 5.2226 | 482.224 | 0 | 784.3684 | 0 |
| 50.9147 | 0 | 216.897 | 0 | 585.1803 | 25.4609 | 784.4365 | 18.3544 |
| 53.2002 | 0 | 218.1313 | 11.6504 | 585.2159 | 0 | 798.4154 | 112.0094 |
| 55.3069 | 0.3144 | 218.4937 | 0 | 588.9885 | 0 | 801.8206 | 0 |
| 56.3097 | 0 | 226.7978 | 4.7359 | 589.0536 | 21.5489 | 806.6279 | 169.7447 |
| 59.1625 | 5.991 | 226.9038 | 0 | 592.4738 | 0 | 806.8649 | 0 |
| 59.8489 | 0 | 289.7068 | 0 | 592.4745 | 0.1328 | 807.9775 | 120.8904 |
| 61.5608 | 5.0124 | 289.7116 | 0.0827 | 598.1579 | 26.6417 | 808.0478 | 0 |
| 63.2771 | 0.8748 | 291.2965 | 0 | 598.1992 | 0 | 850.2579 | 0 |
| 63.3703 | 0 | 291.5054 | 0.0912 | 599.2144 | 0 | 850.3431 | 74.6704 |
| 64.3256 | 1.8769 | 297.7133 | 0 | 599.2544 | 21.2304 | 855.7887 | 39.2629 |
| 64.8365 | 0 | 297.9614 | 1.3903 | 609.5693 | 0 | 856.9945 | 0 |
| 65.9391 | 2.4496 | 326.2533 | 0 | 609.707 | 6.4886 | 860.7501 | 56.5966 |
| 67.77 | 0 | 326.257 | 4.2363 | 614.2649 | 56.2976 | 860.8075 | 0 |
| 69.6183 | 0 | 333.3926 | 0 | 614.3472 | 0 | 874.3911 | 0 |
| 74.2641 | 4.8827 | 333.9757 | 4.8618 | 618.3128 | 0 | 874.3951 | 8.7236 |
| 75.2432 | 0 | 335.076 | 8.9796 | 619.3108 | 85.1984 | 875.2409 | 5.9103 |
| 76.0726 | 4.2221 | 335.7368 | 0 | 619.7584 | 52.6792 | 875.2426 | 0 |
| 79.8592 | 0 | 365.5461 | 1.7189 | 619.8212 | 0 | 877.4122 | 0 |
| 80.8216 | 1.4527 | 365.6725 | 0 | 655.3927 | 9.2644 | 877.8359 | 14.8603 |
| 80.8688 | 0 | 373.5711 | 0 | 655.399 | 0 | 898.2481 | 43.774 |
| 81.4978 | 0.2355 | 373.5727 | 0.5468 | 657.5675 | 0 | 898.3571 | 0 |

**Table 5.** (continued)

| Frequency $cm^{-1}$ | Intensity (km/mol) | Frequency $cm^{-1}$ | Intensity (km/mol) | Frequency $cm^{-1}$ | Intensity (km/mol) | Frequency $cm^{-1}$ | Intensity (km/mol) |
|---|---|---|---|---|---|---|---|
| 898.9678 | 114.2656 | 1249.6028 | 0 | 1384.7289 | 0 | 1673.2216 | 1253.6383 |
| 899.6584 | 0 | 1252.2239 | 0 | 1386.7623 | 54.0952 | 1677.5648 | 254.4055 |
| 903.7786 | 0 | 1253.5337 | 140.7511 | 1386.9449 | 0 | 1677.5771 | 0 |
| 903.7878 | 40.4836 | 1259.2854 | 0 | 1387.2804 | 311.9294 | 1696.2489 | 0 |
| 925.1438 | 0 | 1259.7135 | 74.642 | 1387.6086 | 0 | 1696.2622 | 751.9892 |
| 925.2002 | 292.8446 | 1268.1906 | 19.3053 | 1387.6719 | 13.3364 | 1698.1921 | 0 |
| 931.0855 | 649.434 | 1268.2472 | 0 | 1414.9059 | 44.1271 | 1698.2057 | 641.3516 |
| 931.3673 | 0 | 1268.922 | 47.0974 | 1414.9625 | 0 | 3023.3391 | 21.6024 |
| 937.9984 | 0 | 1268.9448 | 0 | 1418.0494 | 65.8201 | 3023.3445 | 0 |
| 941.9125 | 342.7514 | 1273.0648 | 142.252 | 1418.2875 | 0 | 3027.7644 | 0 |
| 947.154 | 0 | 1273.0767 | 0 | 1419.486 | 1.4432 | 3027.7686 | 39.5879 |
| 948.7826 | 415.3135 | 1275.387 | 0 | 1419.5223 | 0 | 3038.7473 | 16.1057 |
| 950.1349 | 316.6856 | 1275.6105 | 233.769 | 1425.1407 | 235.0826 | 3038.76 | 0 |
| 950.1881 | 0 | 1278.2577 | 0 | 1425.2646 | 0 | 3043.4661 | 31.0481 |
| 954.576 | 453.1379 | 1278.3093 | 103.4302 | 1429.217 | 0 | 3043.5422 | 0 |
| 955.4264 | 0 | 1281.2936 | 0 | 1431.4359 | 198.5826 | 3062.6191 | 8.9564 |
| 966.3974 | 0 | 1281.2948 | 11.3502 | 1434.2299 | 374.2726 | 3062.6216 | 0 |
| 966.5695 | 114.222 | 1301.0441 | 0 | 1435.7983 | 0 | 3066.1562 | 0 |
| 969.9396 | 0 | 1302.1788 | 192.7808 | 1457.8159 | 193.8634 | 3066.1794 | 3.3107 |
| 971.1288 | 151.9144 | 1309.0847 | 272.2128 | 1458.1257 | 0 | 3102.0098 | 10.9209 |
| 975.6687 | 0 | 1309.2377 | 0 | 1461.3976 | 17.8474 | 3102.01 | 0 |
| 977.1353 | 79.7326 | 1312.2554 | 286.1903 | 1461.6547 | 0 | 3107.6062 | 0 |
| 1024.5593 | 0 | 1312.9231 | 0 | 1475.097 | 0 | 3107.616 | 3.8956 |
| 1024.5771 | 377.1222 | 1313.1992 | 646.2577 | 1475.1646 | 47.3409 | 3107.6624 | 3.542 |
| 1048.7135 | 0 | 1314.6346 | 0 | 1483.7729 | 0 | 3107.6665 | 0 |
| 1049.1174 | 53.5188 | 1315.3098 | 0 | 1483.7754 | 12.9222 | 3218.8779 | 0 |
| 1049.3091 | 0 | 1316.0811 | 913.8702 | 1484.8417 | 13.8735 | 3218.916 | 24.4439 |
| 1049.5686 | 62.0334 | 1319.2419 | 0 | 1484.9602 | 0 | 3221.4097 | 0 |
| 1052.6927 | 0 | 1319.7644 | 924.3799 | 1486.7303 | 0 | 3221.446 | 20.7949 |
| 1053.12 | 0 | 1345.8979 | 0 | 1486.8969 | 5.6923 | 3223.0161 | 33.62 |
| 1053.575 | 179.892 | 1346.0634 | 71.0266 | 1498.8737 | 48.683 | 3223.0215 | 0 |
| 1054.0551 | 361.5399 | 1349.5865 | 0 | 1499.1572 | 0 | 3223.2288 | 24.2489 |
| 1061.5616 | 0 | 1350.8397 | 193.1595 | 1499.9746 | 115.5259 | 3223.2302 | 0 |
| 1062.9187 | 391.2202 | 1353.7626 | 0 | 1500.0326 | 0 | 3224.6284 | 0 |
| 1150.3763 | 0 | 1354.9556 | 76.9966 | 1506.8451 | 67.5683 | 3224.6299 | 19.9438 |
| 1150.3794 | 4.4718 | 1364.2341 | 0 | 1506.8896 | 0 | 3224.7954 | 28.5898 |
| 1162.2494 | 3.9166 | 1364.2791 | 32.2566 | 1610.8904 | 60.472 | 3224.8069 | 0 |
| 1162.2515 | 0 | 1367.2747 | 0 | 1613.2507 | 0 | 3230.7817 | 0 |
| 1166.319 | 0 | 1367.5415 | 41.3065 | 1615.5862 | 0 | 3230.7827 | 20.5267 |
| 1166.3846 | 1.5789 | 1369.2303 | 0 | 1618.7401 | 690.5589 | 3231.4448 | 27.0212 |
| 1240.6893 | 135.2084 | 1369.3582 | 57.0854 | 1640.0295 | 0 | 3231.4531 | 0 |
| 1240.8419 | 0 | 1369.6066 | 0 | 1645.7317 | 96.8361 | 3237.3953 | 0 |
| 1241.6234 | 46.6453 | 1369.7725 | 67.5151 | 1646.9904 | 0 | 3237.4807 | 113.038 |
| 1241.6421 | 0 | 1377.9336 | 0 | 1653.692 | 478.6351 | | |
| 1243.2505 | 0 | 1379.5659 | 200.2331 | 1666.0964 | 0 | | |
| 1243.2968 | 46.997 | 1380.469 | 84.0733 | 1666.4061 | 67.5463 | | |
| 1249.5413 | 75.4649 | 1380.4916 | 0 | 1672.3979 | 0 | | |

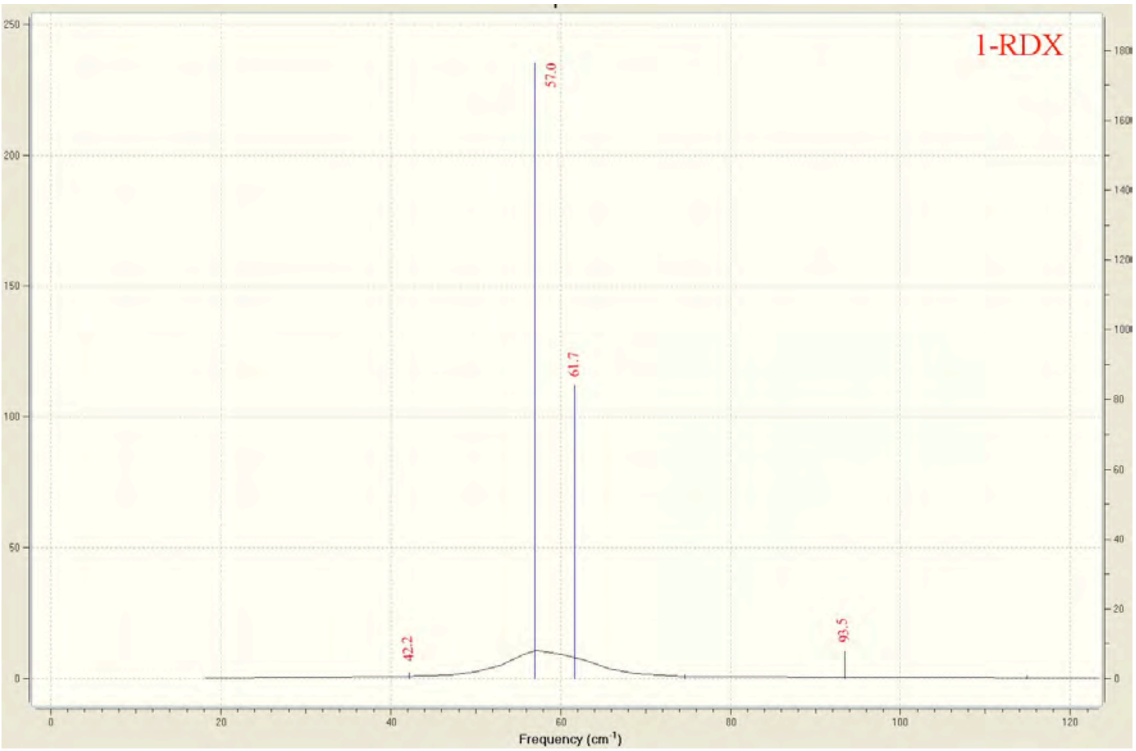


Figure 6. IR intensity as a function of frequency calculated using DFT B3LYP/6-311G(2d,2p) for single isolated molecule of RDX according to frozen phonon approximation.

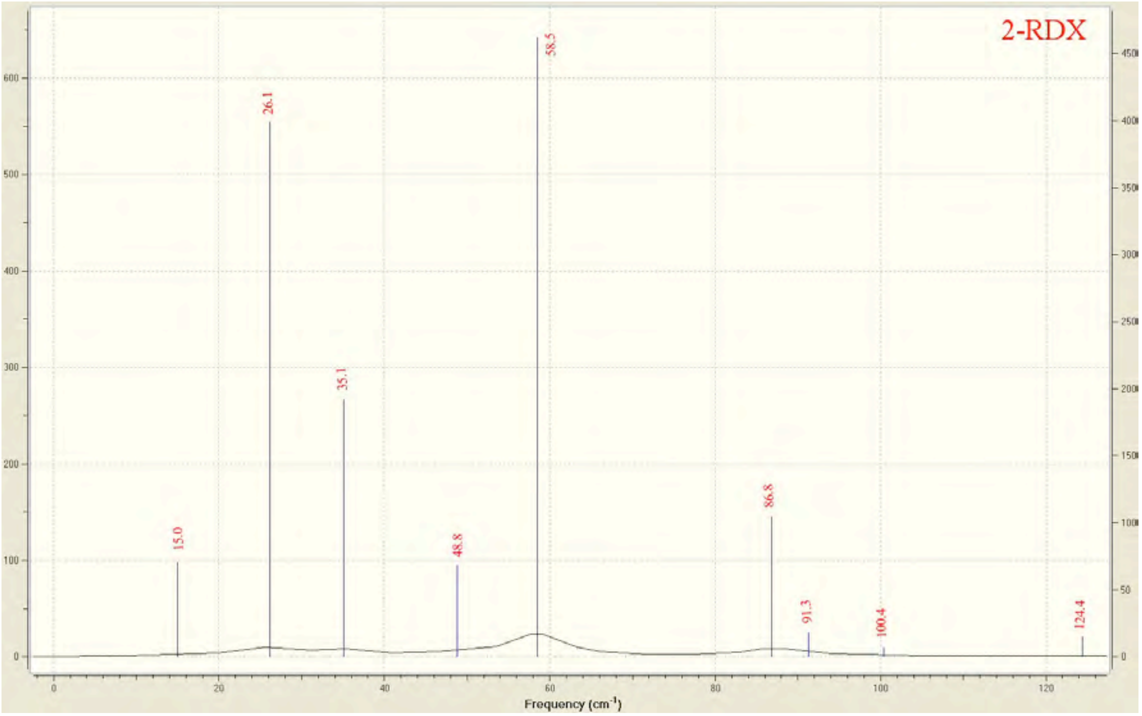


Figure 7. IR intensity as a function of frequency calculated using DFT B3LYP/6-311G(2d,2p) for two-molecule cluster of RDX according to frozen phonon approximation.

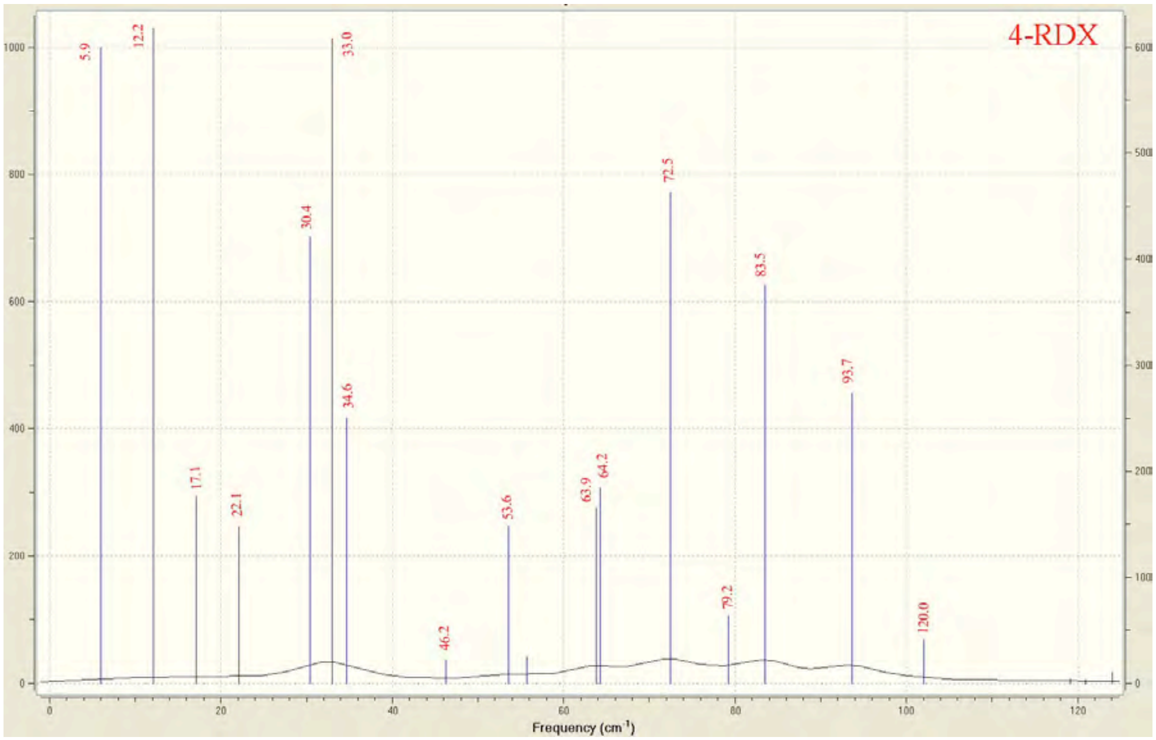


Figure 8. IR intensity as a function of frequency calculated using DFT B3LYP/6-311G(2d,2p) for four-molecule cluster of RDX according to frozen phonon approximation.

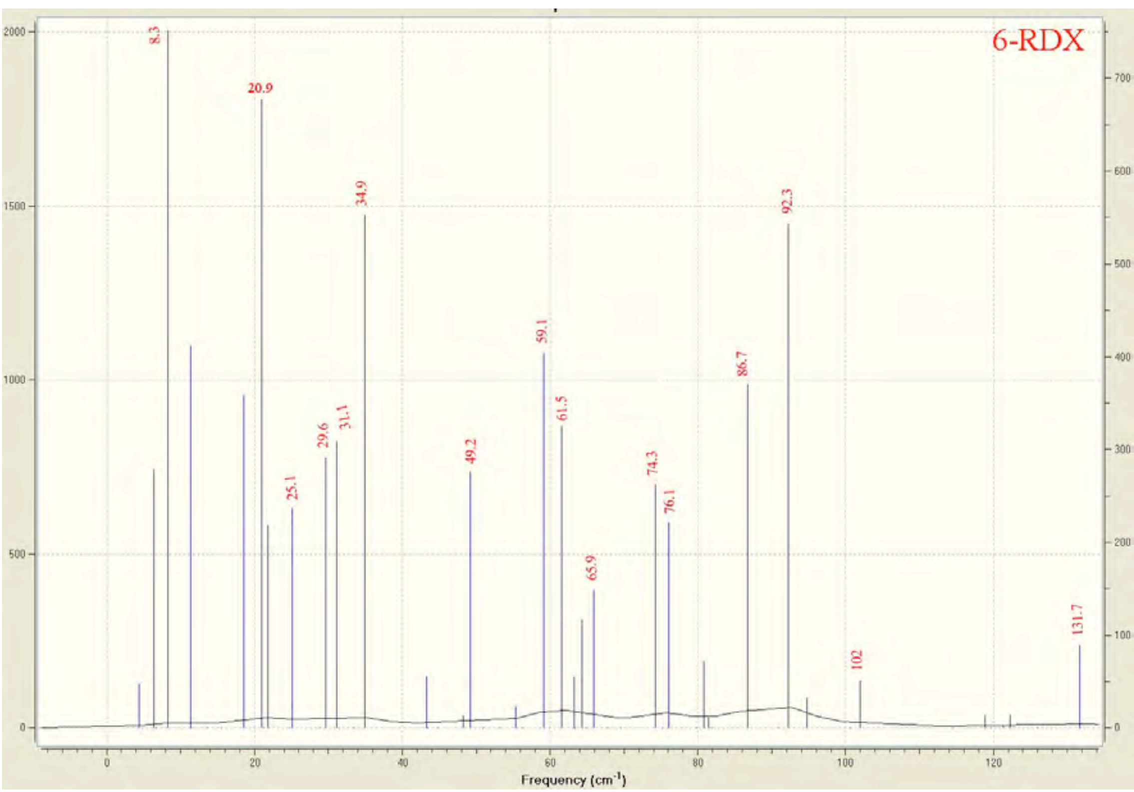


Figure 9. IR intensity as a function of frequency calculated using DFT B3LYP/6-311G(2d,2p) for six-molecule cluster of RDX according to frozen phonon approximation.

Shown in Figs. 10 and 11 are spectra of clusters in comparison with experimentally measured spectra [19, 20]. Referring to these figures, initial consideration is given to what extent various average features of the DFT calculated spectra for different size molecular clusters, as well as experimentally measured spectra, are correlated with each other. Referring to Fig. 10, one observes on average a noticeable correlation between DFT calculated spectra for molecule clusters of RDX and experimentally measured spectrum for dielectric response of RDX solid. The comparison of spectra shown in Fig. 10 also supports the notion that certain resonance features, which are associated with finite-size molecular clusters, are preserved within clusters of increasing size, as well as in solid form, thus implying a persistence of these modes after coupling to intermolecular influences. The persistence of certain intramolecular modes, which is irrespective of molecular cluster size, i.e., whether the molecule is isolated, part of a cluster or within a bulk lattice, is demonstrated by comparison of DFT calculated and experimentally measured spectra. Shown in Shown in Table 6 is a comparison of DFT calculated frequencies corresponding to prominent absorptions, which have been observed experimentally for RDX in solid state. Referring to this table, one can observe a high correlation between DFT calculated spectra for different cluster sizes and experimentally determined absorption lines at the specific frequencies indicated.

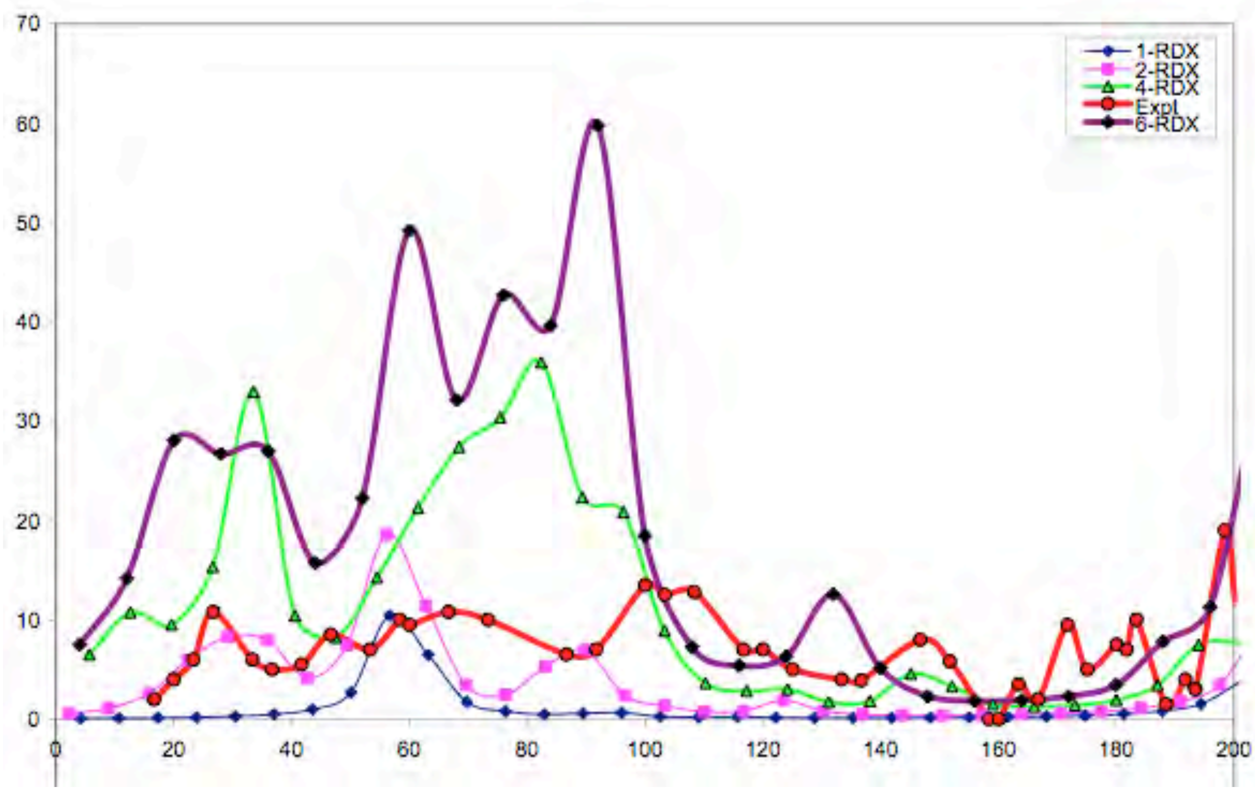


Figure 10. Qualitative comparison of DFT calculated spectra for 1-, 2-, 4- and 6-molecule clusters of RDX and experimentally measured spectrum for dielectric response of RDX solid.

**Table 6.** Comparison of DFT calculated and experimentally measured frequencies at prominent absorptions for RDX solid [19].

| Exp ($cm^{-1}$) | 27 | 35 | 46 | 51 | 66 | 74 | 103 |
|---|---|---|---|---|---|---|---|
| 1-RDX | - | - | 42 | 57 | 62 | - | 94 |
| 2-RDX | 26 | 35 | 49 | 59 | - | 87 | 100 |
| 4-RDX | 17-22 | 33 | 46 | 54 | 64 | 73 | 84-94 |
| 6-RDX | 21 | 35 | 49 | 59 | 66 | 74 | 92 |

Referring to Fig. 11, one observes on average a noticeable correlation between DFT calculated spectra for molecule clusters of RDX and experimentally measured spectrum for dielectric response of RDX vapor. Shown in Shown in Table 7 is a comparison of DFT calculated frequencies corresponding to prominent absorptions, which have been observed experimentally for RDX in vapor state. Referring to this table, one can observe a high correlation between DFT calculated spectra for different cluster sizes and experimentally determined absorption lines at the specific frequencies indicated.

**Table 7.** Comparison of DFT calculated and experimentally measured frequencies at prominent absorptions for RDX vapor [20].

| Exp ($cm^{-1}$) | 1272 | 1602 |
|---|---|---|
| 1-RDX | 1310 | 1663-1701 |
| 2-RDX* | 1306 | 1677 |
| 4-RDX* | 1314 | 1696 |
| 6-RDX* | 1316 | 1673 |

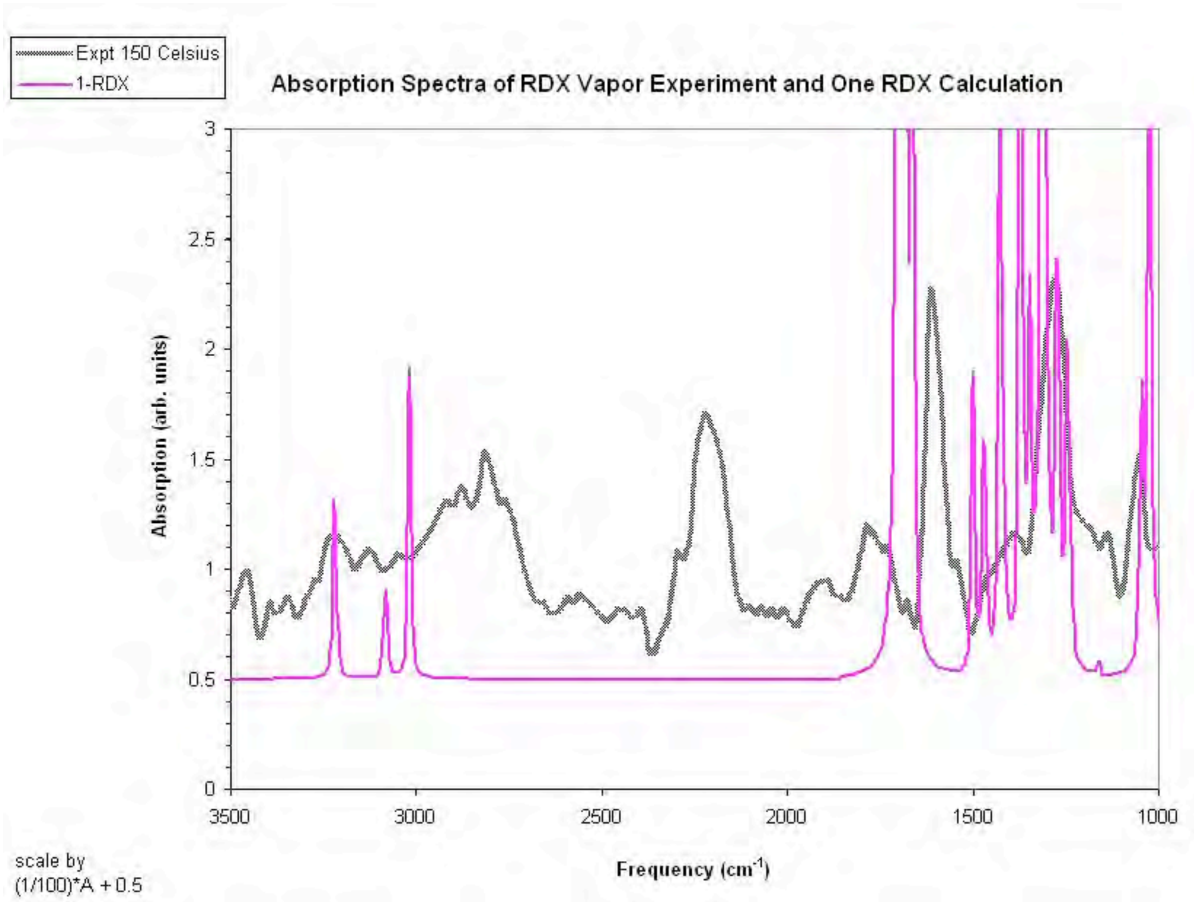


Figure 11(a). Qualitative comparison of DFT calculated spectra for single isolated molecule of RDX and experimentally measured spectrum for dielectric response of RDX vapor.

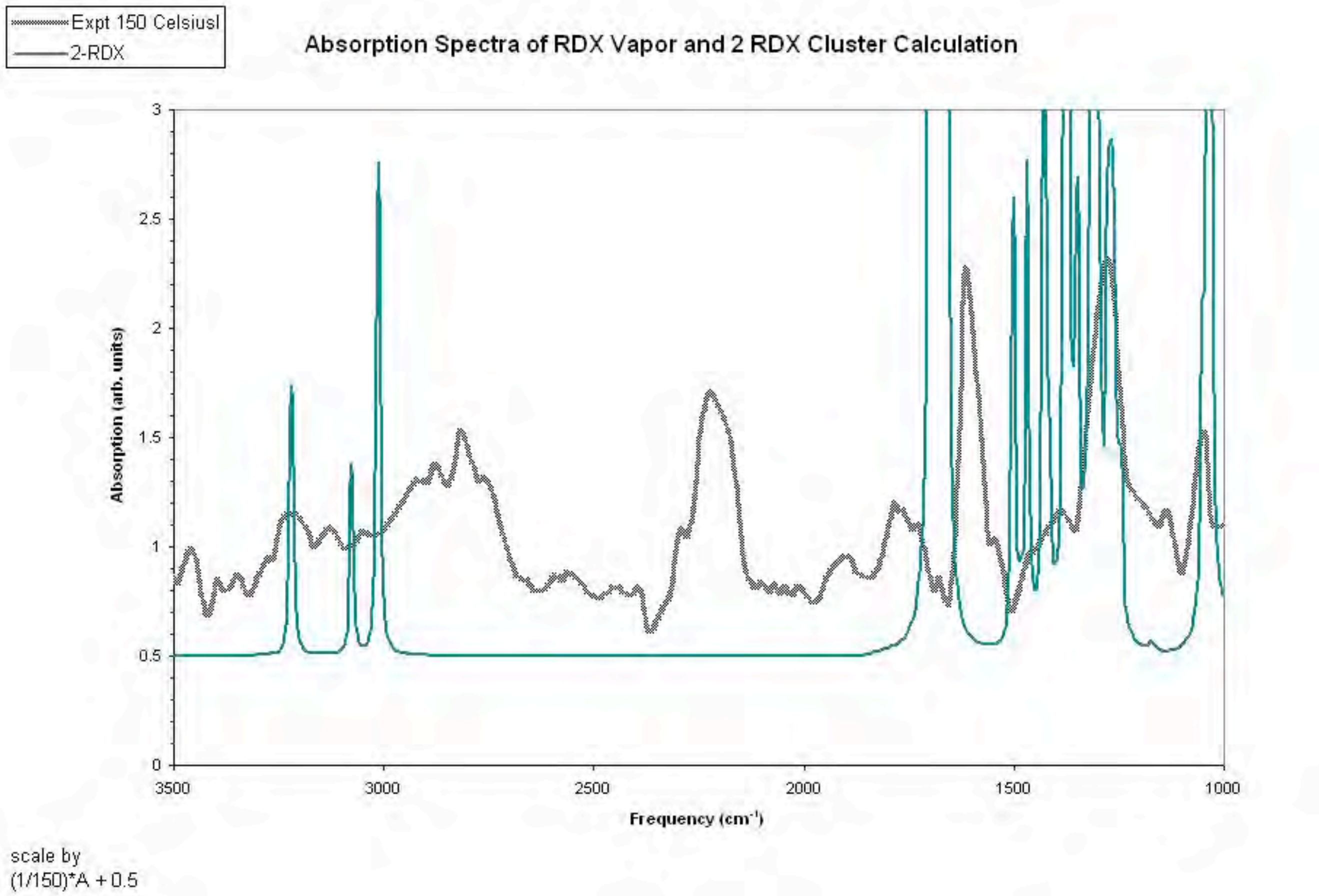


Figure 11(b). Qualitative comparison of DFT calculated spectra for 2-molecule cluster of RDX and experimentally measured spectrum for dielectric response of RDX vapor.

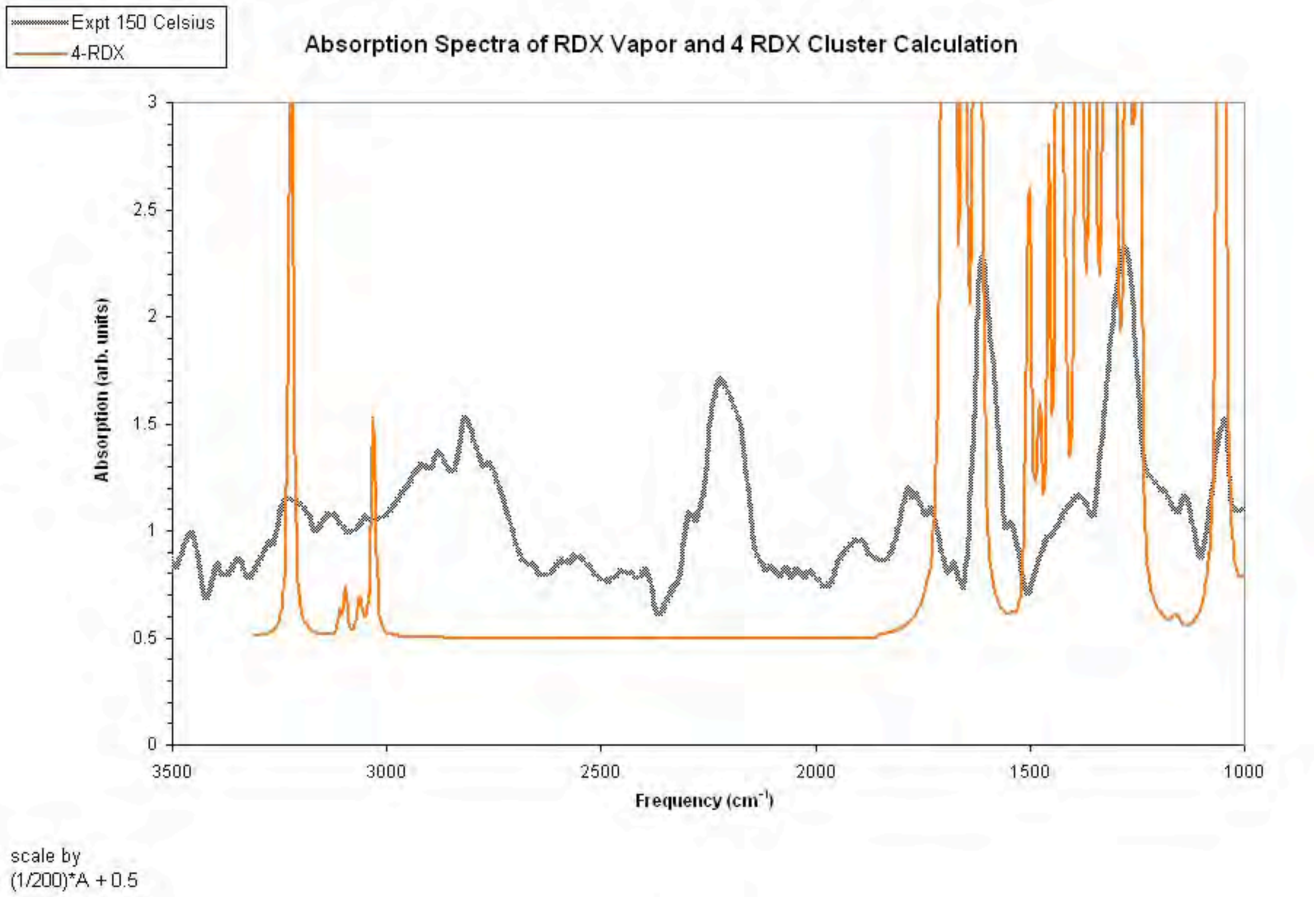


Figure 11(c). Qualitative comparison of DFT calculated spectra for 4-molecule cluster of RDX and experimentally measured spectrum for dielectric response of RDX vapor.

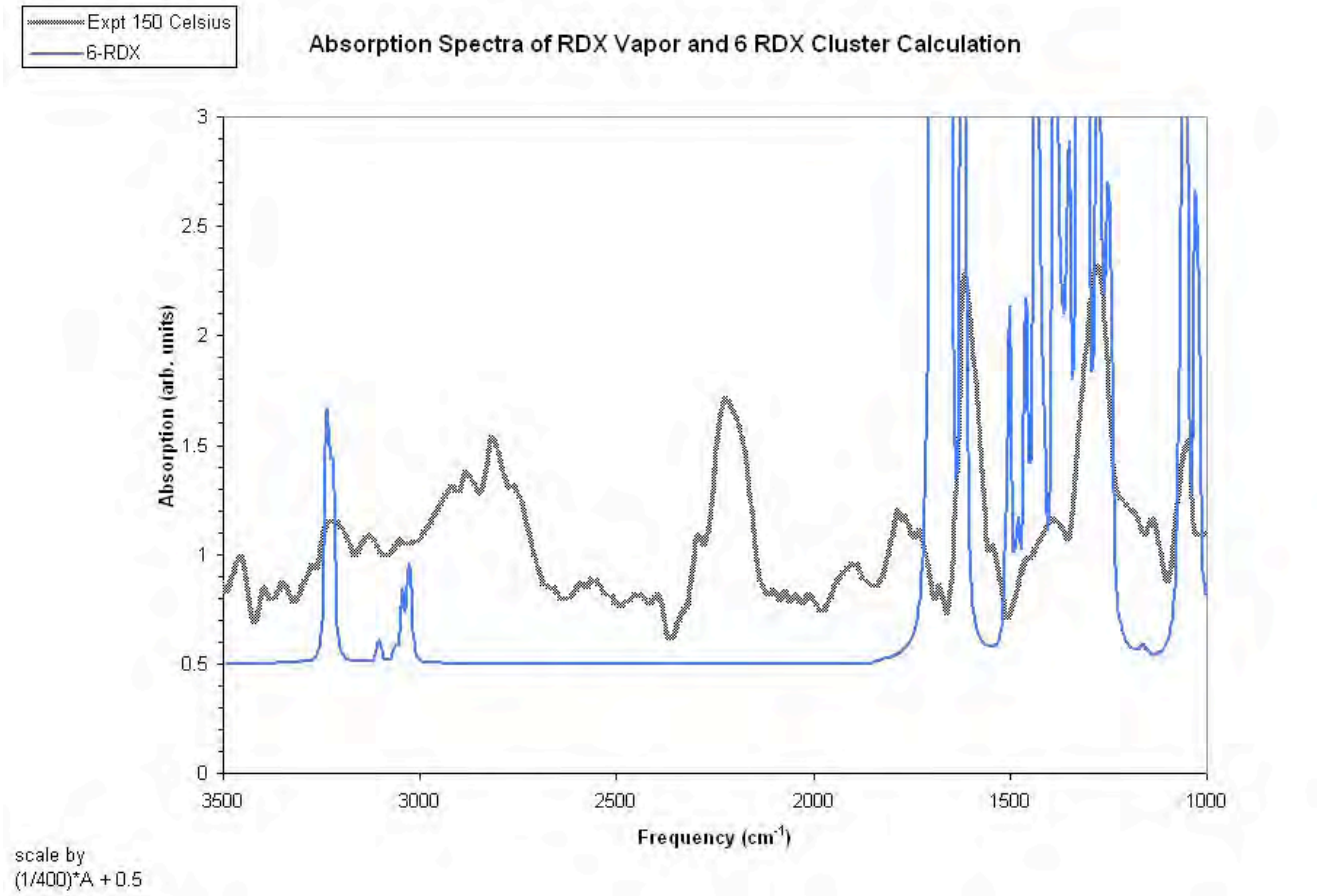


Figure 11(d). Qualitative comparison of DFT calculated spectra for 6-molecule cluster of RDX and experimentally measured spectrum for dielectric response of RDX vapor.

**Ground State Resonance Structure of 3-Molecule Cluster of PETN**

In this section are presented the results of computational experiments using DFT concerning 3-molecule cluster of PETN. These results include the relaxed or equilibrium configuration of a single isolated molecule of PETN (see Table 8) and ground-state oscillation frequencies and IR intensities for this configuration, which are calculated by DFT according to the frozen phonon approximation (see Table 9). The ground state resonance structure for a single isolated molecule of PETN is adopted as a reference for analysis of spectral features associated with a 3-molecule cluster. For these calculations geometry optimization and vibrational analysis was effected using the DFT model B3LYP [12, 13] and basis function 6-311G(2d,2p) [14,15]. According to the specification of this basis function, (2d,2p) designates polarization functions having 2 sets of d functions for heavy atoms and 2 sets of p functions for hydrogen atoms [16]. A schematic representation of the molecular geometry of a single isolated molecule of PETN is shown in Fig.(12). A schematic representation of the molecular geometry of a molecular cluster consisting of 3 molecules is shown in Figs. (13). It is significant to note that the relative positions of the molecules associated with this molecular cluster are according to crystallographic structure conditions that would be associated with bulk material. In particular, the crystal structure of PETN, whose CCDC reference code is PEYTN01, has been investigated by H. H. Cady, A. C. Larson (1975) [21]. The space group for this crystal structure is ***Pcnb*** (symmetry operators are x, y, z; ½-x, y, ½+z; ½+x, ½-y, ½+z; -x, ½-y, z; -x, -y, -z; ½+x, -y, ½-z; ½-x, ½+y, ½-z; x, ½+y, -z), and the unit cell constants are a=13.290, b=13.490, c=6.830, $\alpha$=90.00, $\beta$=90.00, $\gamma$=90.00 and density 1.715 g/cm$^3$. The ground-state oscillation frequencies and IR intensities for the 3-molecule cluster of PETN, corresponding to its relaxed equilibrium configuration, are calculated by DFT according to the frozen phonon approximation. In the case of a molecular cluster of 3 molecules, these values are given in Table 10. The DFT model and basis function used for these calculations are the same as those used for the single isolated molecule of PETN.

**Table 8.** Atomic positions of PETN (Å) after optimization.

| Atomic number | X | Y | Z | Atomic number | X | Y | Z |
|---|---|---|---|---|---|---|---|
| 6 | -0.89008 | 0.487044 | 0.169443 | 8 | 1.885603 | -3.148164 | -0.06536 |
| 6 | 0.56833 | 0.025631 | 0.355901 | 8 | 2.801652 | -1.246607 | 0.487954 |
| 6 | -0.954153 | 2.010353 | 0.393203 | 1 | -1.969444 | 2.373078 | 0.253141 |
| 6 | -1.775405 | -0.266852 | 1.180709 | 1 | -0.289344 | 2.531375 | -0.29121 |
| 6 | -1.399001 | 0.17896 | -1.25209 | 1 | 0.903906 | 0.201954 | 1.374781 |
| 8 | -0.536524 | 2.246621 | 1.753563 | 1 | 1.224466 | 0.550575 | -0.333979 |
| 8 | 0.594489 | -1.388358 | 0.071682 | 1 | -1.43301 | -0.084138 | 2.196278 |
| 8 | -3.114945 | 0.243543 | 1.019535 | 1 | -1.763653 | -1.336176 | 0.985073 |
| 8 | -0.503707 | 0.845656 | -2.165744 | 1 | -2.410743 | 0.55161 | -1.391197 |
| 8 | -5.169236 | 0.102355 | 1.756224 | 1 | -1.382201 | -0.89204 | -1.438315 |
| 8 | -3.660475 | -1.176108 | 2.678384 | 7 | -4.069163 | -0.341502 | 1.911776 |
| 8 | -0.213539 | 3.790051 | 3.268901 | 7 | -0.561634 | 3.625752 | 2.13612 |
| 8 | -0.916392 | 4.418249 | 1.301021 | 7 | 1.895046 | -1.976796 | 0.177844 |
| 8 | -0.065066 | 1.202636 | -4.278301 | 7 | -0.825239 | 0.640236 | -3.54537 |
| 8 | -1.784867 | -0.046988 | -3.786458 | | | | |

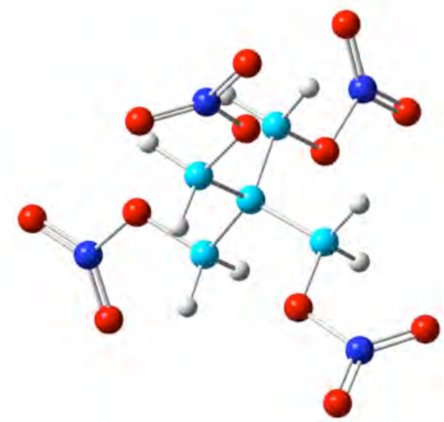

**Figure 12.** Molecular Geometry of PETN

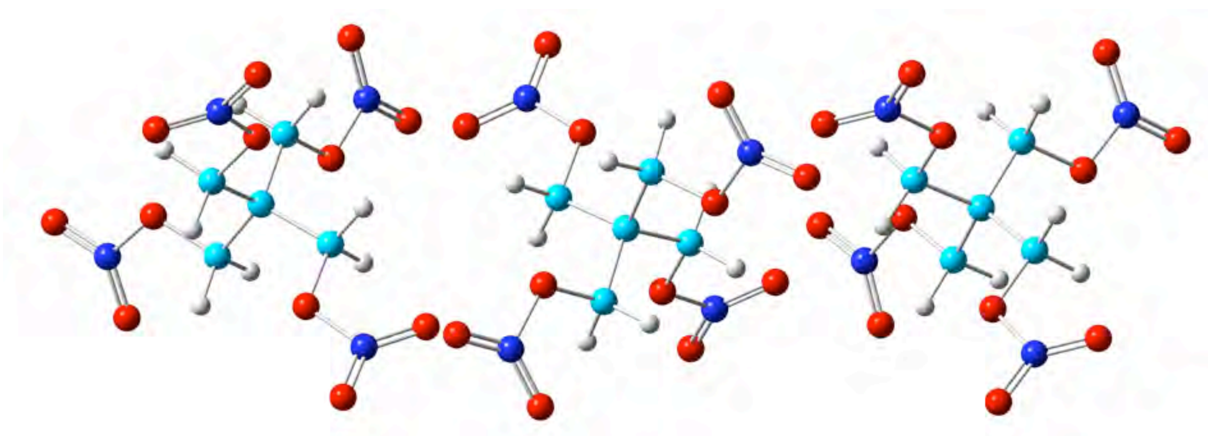

**Figure 13.** Molecular Geometry of 3-Moleculae Cluster of PETN

Proceeding, shown in Figs. 14 and 15 are calculated IR intensities for a single isolated molecule and 3-molecule cluster of PETN. Shown in Figs. 16 and 17, are continuous spectra consisting of a superposition of essentially Lorenzian functions of various heights and widths, which have been constructed using the discrete spectra given in Tables 9 and 10, respectively.

**Table 9.** Oscillation frequencies and IR intensities for single isolated molecule of PETN.

| Frequency $cm^{-1}$ | Intensity (km/mol) | Frequency $cm^{-1}$ | Intensity (km/mol) | Frequency $cm^{-1}$ | Intensity (km/mol) | Frequency $cm^{-1}$ | Intensity (km/mol) |
|---|---|---|---|---|---|---|---|
| 23.0186 | 0 | 319.7365 | 0 | 927.126 | 12.2082 | 1410.9192 | 64.19 |
| 23.468 | 1.7622 | 453.5805 | 3.6627 | 944.6012 | 7.5925 | 1425.4355 | 0 |
| 37.0668 | 0.0792 | 453.5809 | 3.6627 | 944.6018 | 7.5925 | 1513.7205 | 0 |
| 38.2553 | 1.0181 | 533.9816 | 12.509 | 1015.2359 | 0 | 1514.457 | 4.0158 |
| 38.256 | 1.0182 | 589.553 | 0 | 1031.1128 | 68.9949 | 1520.2629 | 13.4384 |
| 49.1445 | 0 | 620.4669 | 9.0561 | 1031.1133 | 68.9954 | 1520.2631 | 13.4385 |
| 51.2098 | 0.0198 | 625.7476 | 8.654 | 1063.903 | 0 | 1765.1326 | 0 |
| 56.1273 | 1.4445 | 625.7479 | 8.6542 | 1069.3729 | 100.3831 | 1766.3812 | 231.1996 |
| 56.1281 | 1.4444 | 676.3956 | 0 | 1184.1914 | 2.4068 | 1767.5533 | 544.1035 |
| 125.0831 | 0.5041 | 711.7268 | 53.505 | 1203.243 | 0.1994 | 1767.554 | 544.1009 |
| 125.0838 | 0.5041 | 711.7271 | 53.5047 | 1203.2433 | 0.1994 | 3081.5559 | 5.7489 |
| 137.2362 | 0.8057 | 756.1322 | 54.9232 | 1264.3964 | 0 | 3082.5044 | 7.1942 |
| 149.3 | 0 | 775.0616 | 12.1352 | 1284.5981 | 21.2105 | 3082.5051 | 7.1942 |
| 175.381 | 0 | 775.0623 | 12.1353 | 1284.5988 | 21.2112 | 3084.4409 | 0 |
| 198.2257 | 0.822 | 775.6437 | 0 | 1310.0272 | 243.6025 | 3139.0088 | 0 |
| 198.2262 | 0.822 | 776.5314 | 30.3068 | 1329.7418 | 272.2731 | 3140.7324 | 5.4891 |
| 213.1381 | 0 | 842.7866 | 0 | 1329.7419 | 272.2725 | 3140.7327 | 5.4894 |
| 253.3021 | 2.0613 | 857.2537 | 365.5689 | 1343.2953 | 0 | 3143.0876 | 10.9428 |
| 256.0704 | 1.9542 | 857.2545 | 365.5689 | 1344.2228 | 196.2847 | | |
| 256.0709 | 1.9542 | 861.1535 | 708.764 | 1406.7094 | 43.0983 | | |
| 309.178 | 1.5099 | 887.0866 | 0 | 1406.7097 | 43.0982 | | |

**Table 10.** Oscillation frequencies and IR intensities for 3-molecule cluster of PETN.

| Frequency $cm^{-1}$ | Intensity (km/mol) | Frequency $cm^{-1}$ | Intensity (km/mol) | Frequency $cm^{-1}$ | Intensity (km/mol) | Frequency $cm^{-1}$ | Intensity (km/mol) |
|---|---|---|---|---|---|---|---|
| 2.7459 | 0.005 | 143.6774 | 0.09 | 625.2445 | 1.4605 | 939.29 | 0.062 |
| 3.0959 | 0 | 150.8196 | 0 | 625.2576 | 16.8618 | 942.0798 | 0.9418 |
| 5.9927 | 0 | 151.0548 | 0.6581 | 630.3136 | 20.158 | 942.9281 | 15.3538 |
| 9.3696 | 0.0003 | 151.6617 | 0 | 630.4765 | 2.2566 | 948.6176 | 15.6586 |
| 9.4769 | 0.0102 | 179.9747 | 0.0565 | 633.2105 | 21.9922 | 948.6245 | 2.9713 |
| 12.6516 | 0.0555 | 179.9893 | 0.091 | 677.9521 | 2.6767 | 950.0091 | 9.2565 |
| 19.0972 | 0.6809 | 187.9166 | 0.0943 | 677.9772 | 0.5639 | 1013.7078 | 0.5689 |
| 21.5863 | 0.0499 | 191.0116 | 1.1948 | 679.5992 | 1.3293 | 1014.4844 | 1.6776 |
| 23.4909 | 3.1816 | 193.9818 | 4.2534 | 711.3558 | 37.4622 | 1014.6168 | 1.0282 |
| 24.2182 | 0.0223 | 193.9882 | 0.0045 | 711.5214 | 0.0131 | 1021.6065 | 38.8561 |
| 24.2957 | 0.1038 | 203.0462 | 1.4143 | 711.6724 | 135.8772 | 1026.3538 | 0.189 |
| 26.1885 | 0.0298 | 203.1005 | 0.0342 | 714.8454 | 67.0988 | 1026.4937 | 140.2393 |
| 27.792 | 0.0928 | 204.4253 | 0.2964 | 714.9153 | 4.0388 | 1033.9843 | 152.6453 |
| 29.53 | 0.6686 | 215.1988 | 0.0063 | 717.5967 | 55.4965 | 1034.1356 | 0.5469 |
| 32.3744 | 0.148 | 215.2201 | 0.0489 | 754.8807 | 8.6665 | 1036.3997 | 108.9989 |
| 33.728 | 0.6131 | 216.7523 | 0.0112 | 755.7139 | 6.5923 | 1060.5533 | 11.1806 |
| 36.5112 | 0.1353 | 253.5204 | 2.5784 | 755.9681 | 125.2554 | 1063.3865 | 1.689 |
| 37.9722 | 1.142 | 253.5395 | 1.3166 | 771.4876 | 35.9297 | 1063.7787 | 52.3445 |
| 40.1106 | 0.1238 | 255.4469 | 2.9787 | 771.5766 | 0.5576 | 1068.8099 | 46.4614 |
| 40.2686 | 0.7434 | 256.9556 | 4.6241 | 772.0193 | 52.9692 | 1069.15 | 1.7564 |
| 40.6739 | 0.0067 | 256.9622 | 0.0114 | 772.045 | 32.2983 | 1070.5229 | 152.8388 |
| 41.148 | 0.0902 | 258.4687 | 2.3891 | 775.0159 | 0.3922 | 1182.1937 | 0.5315 |
| 45.3709 | 0.8009 | 260.5664 | 0.4464 | 775.0287 | 17.1464 | 1183.4821 | 0.5997 |
| 45.4139 | 0.0058 | 260.6916 | 6.0475 | 775.3692 | 5.8581 | 1183.5236 | 3.8764 |
| 49.0572 | 0.1161 | 261.354 | 4.6746 | 775.3761 | 7.2323 | 1200.4976 | 0.5446 |
| 52.0377 | 0.0004 | 308.4312 | 0.5996 | 775.5979 | 15.9024 | 1201.5612 | 1.1979 |
| 52.0415 | 2.3979 | 310.0498 | 1.3298 | 776.2775 | 20.1457 | 1201.5688 | 0.0735 |
| 52.8558 | 0.211 | 310.2897 | 5.5818 | 776.3102 | 0.0334 | 1203.6359 | 0.3577 |
| 54.4623 | 4.7351 | 318.7477 | 0.0604 | 776.7685 | 18.1673 | 1203.7332 | 0.0599 |
| 56.9478 | 1.8936 | 319.4577 | 0.5603 | 843.0367 | 11.9947 | 1203.8767 | 0.012 |
| 56.9559 | 0.0156 | 319.48 | 0.2014 | 843.3959 | 10.8952 | 1264.6515 | 0.0131 |
| 58.1967 | 0.8009 | 452.9283 | 7.3557 | 844.2677 | 3.2431 | 1264.6724 | 1.2153 |
| 59.0884 | 0.0242 | 452.9482 | 0.3582 | 852.5711 | 74.5096 | 1264.6882 | 0 |
| 60.7896 | 0.0144 | 454.1579 | 3.0692 | 854.7542 | 1.2119 | 1284.3719 | 71.0302 |
| 62.0465 | 2.6393 | 456.9975 | 9.8235 | 855.0319 | 1113.0496 | 1284.4592 | 0.0881 |
| 64.1165 | 0.017 | 457.2185 | 0.0887 | 859.1821 | 440.0582 | 1284.9974 | 15.2172 |
| 67.5021 | 2.5334 | 458.9726 | 1.6145 | 859.2446 | 328.521 | 1287.3538 | 49.0979 |
| 81.1563 | 0.063 | 535.0382 | 21.8539 | 862.1922 | 204.4109 | 1287.3636 | 0.2869 |
| 82.4234 | 0.2897 | 535.0643 | 0.3361 | 867.808 | 188.3015 | 1289.071 | 24.2026 |
| 123.768 | 1.6121 | 536.2878 | 2.4334 | 870.1517 | 767.9538 | 1308.4966 | 10.5086 |
| 123.9862 | 0.0784 | 590.701 | 0.0464 | 872.9782 | 442.748 | 1310.3143 | 22.3865 |
| 125.3659 | 0.059 | 590.7104 | 0.044 | 890.1616 | 10.2077 | 1312.6071 | 576.5331 |
| 129.7586 | 0.995 | 591.5033 | 0.0049 | 891.835 | 78.6084 | 1324.9568 | 463.472 |
| 129.8118 | 0.2058 | 621.6932 | 9.3787 | 896.2267 | 265.5877 | 1326.1389 | 650.3981 |
| 140.6045 | 1.3884 | 621.7182 | 2.4644 | 928.7986 | 20.8334 | 1328.1746 | 0.0026 |
| 140.8086 | 0.7455 | 623.7837 | 6.7643 | 928.7987 | 0.2006 | 1330.5981 | 0.0236 |
| 141.5511 | 0.6157 | 624.7261 | 0.1423 | 931.284 | 22.9396 | 1331.6897 | 357.7667 |

**Table 10 (continued)**

| Frequency cm$^{-1}$ | Intensity (km/mol) | Frequency cm$^{-1}$ | Intensity (km/mol) | Frequency cm$^{-1}$ | Intensity (km/mol) | Frequency cm$^{-1}$ | Intensity (km/mol) |
|---|---|---|---|---|---|---|---|
| 1332.6163 | 325.2102 | 1426.7509 | 1.5948 | 1753.121 | 121.7147 | 3095.5657 | 10.7196 |
| 1341.1545 | 0.0623 | 1427.8077 | 0.8237 | 1766.1827 | 656.7066 | 3096.1804 | 2.0796 |
| 1342.6538 | 0.8549 | 1504.132 | 2.0613 | 1766.2982 | 0.0164 | 3098.1538 | 3.8464 |
| 1343.0424 | 2.8398 | 1506.4666 | 40.4544 | 1766.9027 | 527.3882 | 3098.1646 | 1.7708 |
| 1344.1932 | 3.4047 | 1508.4739 | 0.522 | 1767.3317 | 131.9252 | 3136.0608 | 5.0163 |
| 1344.3925 | 9.4586 | 1511.4553 | 16.212 | 1768.5984 | 63.6771 | 3136.0637 | 3.8842 |
| 1344.9041 | 489.2351 | 1512.9001 | 0.4156 | 1769.1071 | 244.2138 | 3140.5251 | 5.7739 |
| 1407.7294 | 75.5986 | 1513.5698 | 2.3789 | 1770.5093 | 937.002 | 3140.7388 | 9.6767 |
| 1407.7589 | 0.0147 | 1513.6084 | 1.62 | 1770.6707 | 151.094 | 3140.7444 | 0.0509 |
| 1408.5706 | 80.8585 | 1516.7607 | 3.007 | 3078.3787 | 9.9733 | 3140.7461 | 5.9203 |
| 1408.7397 | 11.8525 | 1516.7999 | 16.3591 | 3078.3806 | 3.0626 | 3147.1145 | 6.1931 |
| 1408.9039 | 56.6913 | 1518.0491 | 10.1118 | 3079.4727 | 12.1956 | 3147.1213 | 5.1318 |
| 1410.5243 | 34.4459 | 1519.4949 | 21.3927 | 3079.8242 | 1.1214 | 3155.8755 | 4.9167 |
| 1412.4119 | 12.556 | 1519.5026 | 0.0019 | 3081.5474 | 8.191 | 3156.3723 | 4.0165 |
| 1412.4762 | 67.0457 | 1746.3506 | 1019.5118 | 3081.5496 | 2.1684 | 3160.1804 | 3.5558 |
| 1413.4799 | 85.1998 | 1746.6143 | 236.3832 | 3083.6433 | 13.4875 | 3160.1809 | 5.7426 |
| 1426.6968 | 0.2855 | 1752.1338 | 0.2487 | 3083.6489 | 0.0252 | | |

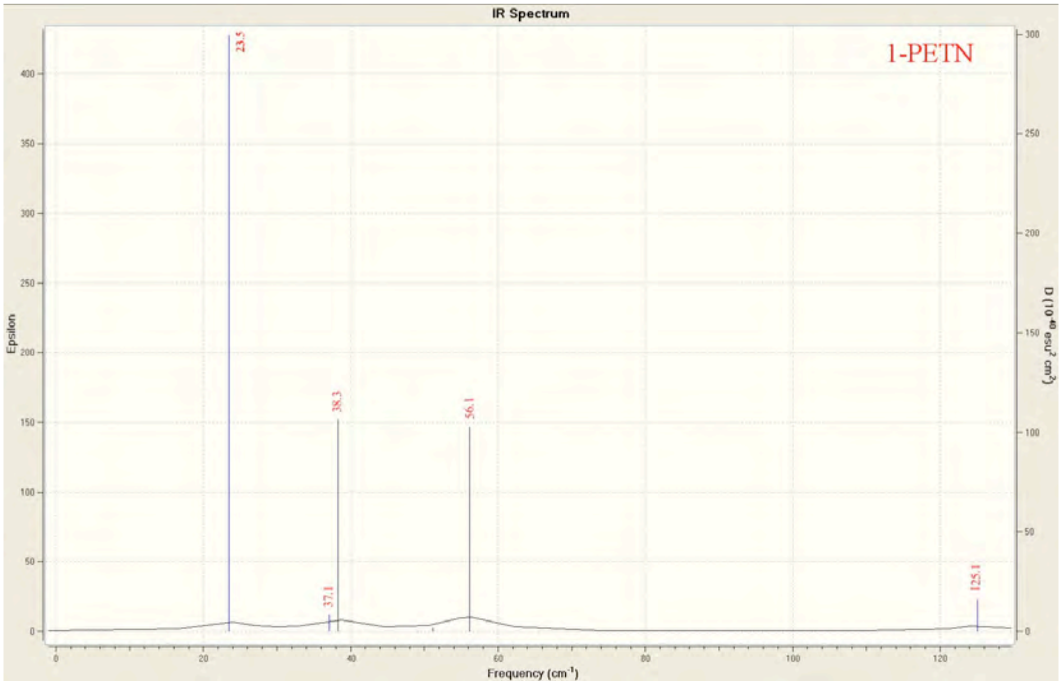


**Figure 14.** IR intensity as a function of frequency calculated using DFT B3LYP/6-311G(2d,2p) for single isolated molecule of PETN according to frozen phonon approximation.

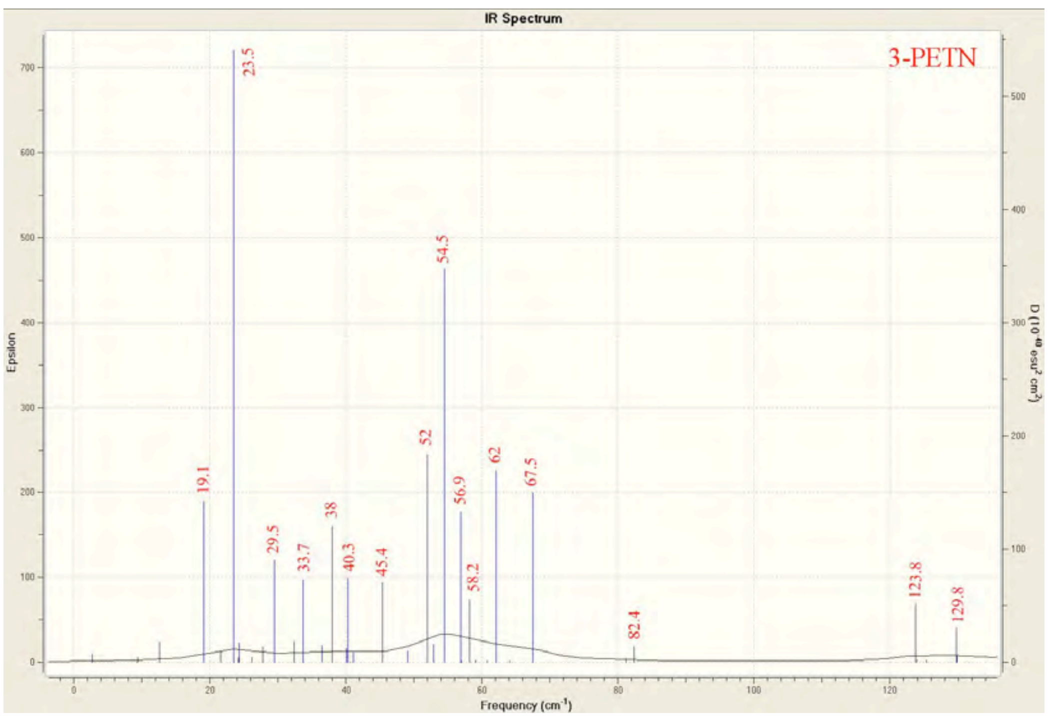


**Figure 15.** IR intensity as a function of frequency calculated using DFT B3LYP/6-311G(2d,2p) for three-molecule cluster of PETN according to frozen phonon approximation.

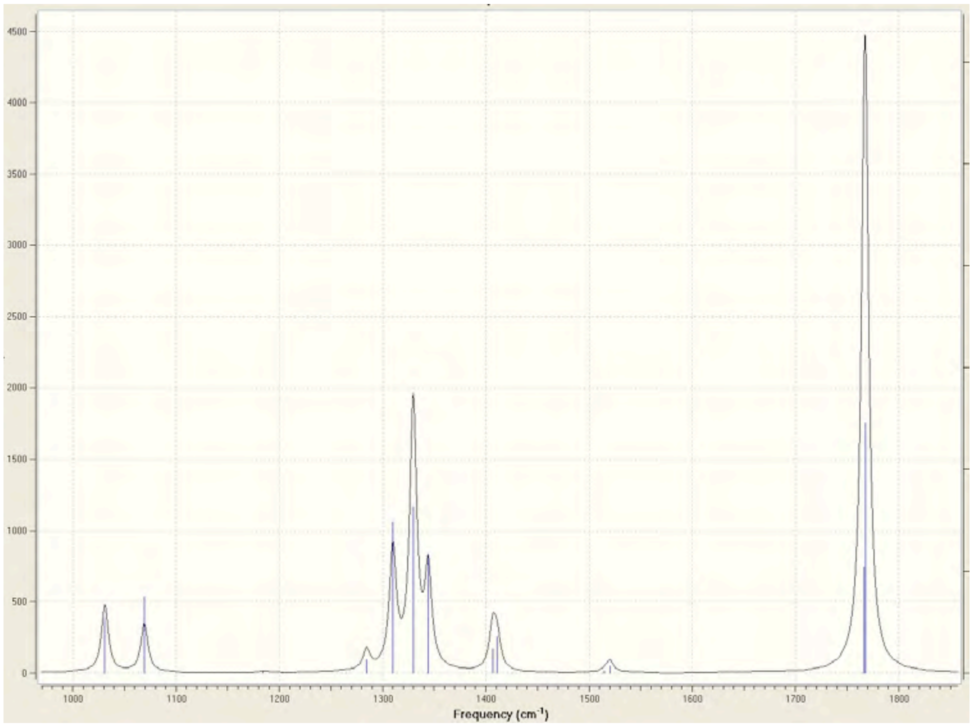


**Figure 16.** Continuous-spectrum representation of IR intensity as a function of frequency calculated using DFT for single isolated molecule of PETN.

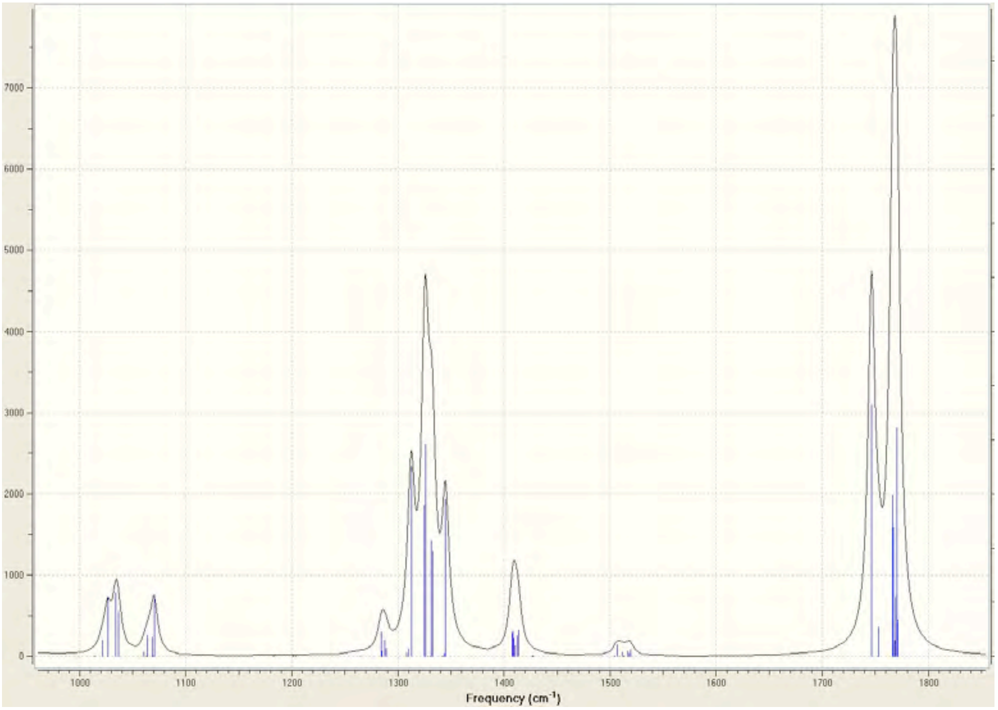


**Figure 17.** Continuous-spectrum representation of IR intensity as a function of frequency calculated using DFT for three-molecule cluster of PETN.

Shown in Figs. 18 and 19 are spectra of clusters in comparison with experimentally measured spectra [19, 20]. Referring to these figures, initial consideration is given to what extent various average features of the DFT calculated spectra for different size molecular clusters, as well as experimentally measured spectra, are correlated with each other. Referring to Fig. 18, one observes on average a noticeable correlation between DFT calculated spectra for molecule clusters of PETN and experimentally measured spectra for the dielectric response of PETN solid. The comparison of spectra shown in Fig. 18 also supports the notion that certain resonance features, which are associated with finite-size molecular clusters, are preserved within clusters of increasing size, as well as in solid form, thus implying a persistence of these modes after coupling to intermolecular influences. The persistence of certain intramolecular modes, which is irrespective of molecular cluster size, i.e., whether the molecule is isolated, part of a cluster or within a bulk lattice, is demonstrated by comparison of DFT calculated and experimentally measured spectra. Shown in Table 11 is a comparison of DFT calculated frequencies corresponding to prominent absorptions, which have been observed experimentally for PETN in solid state. Referring to this table, one can observe a high correlation between DFT calculated spectra for different cluster sizes and experimentally determined absorption lines at the specific frequencies indicated.

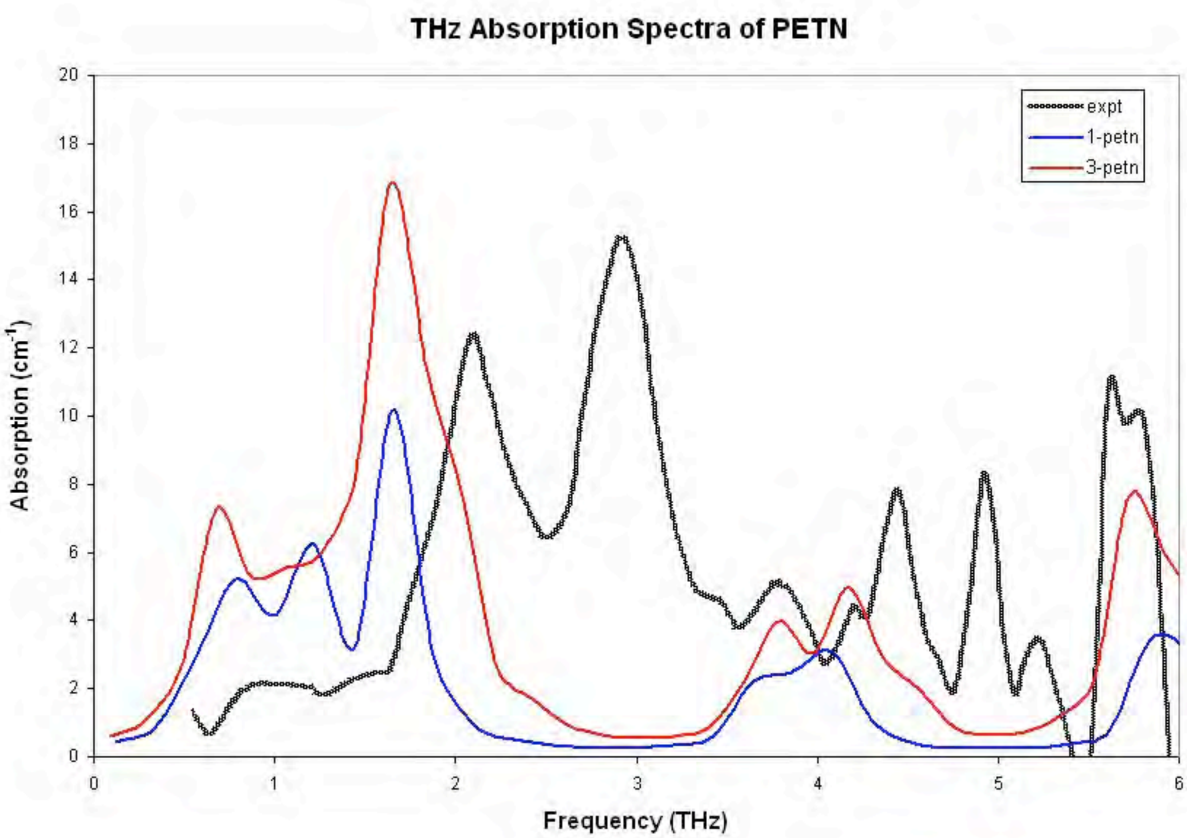


**Figure 18.** Qualitative comparison of DFT calculated spectra for 1-and 3-molecule clusters of PETN and experimentally measured spectrum for dielectric response of PETN solid.

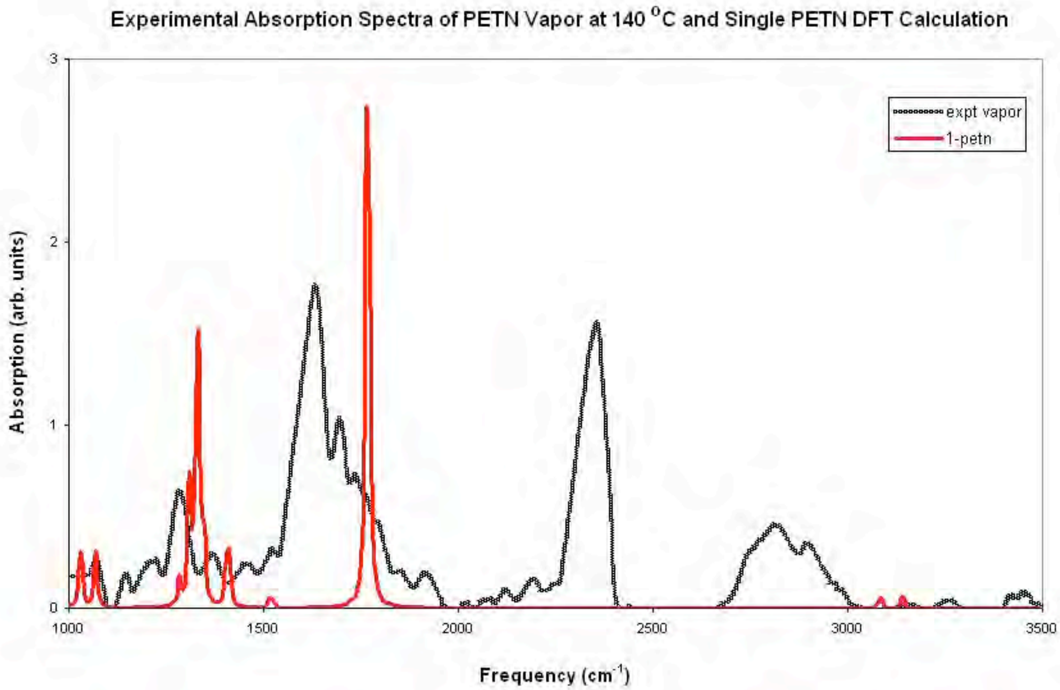


**Figure 19(a).** Qualitative comparison of DFT calculated spectra for single PETN and experimentally measured spectrum for dielectric response of PETN vapor.

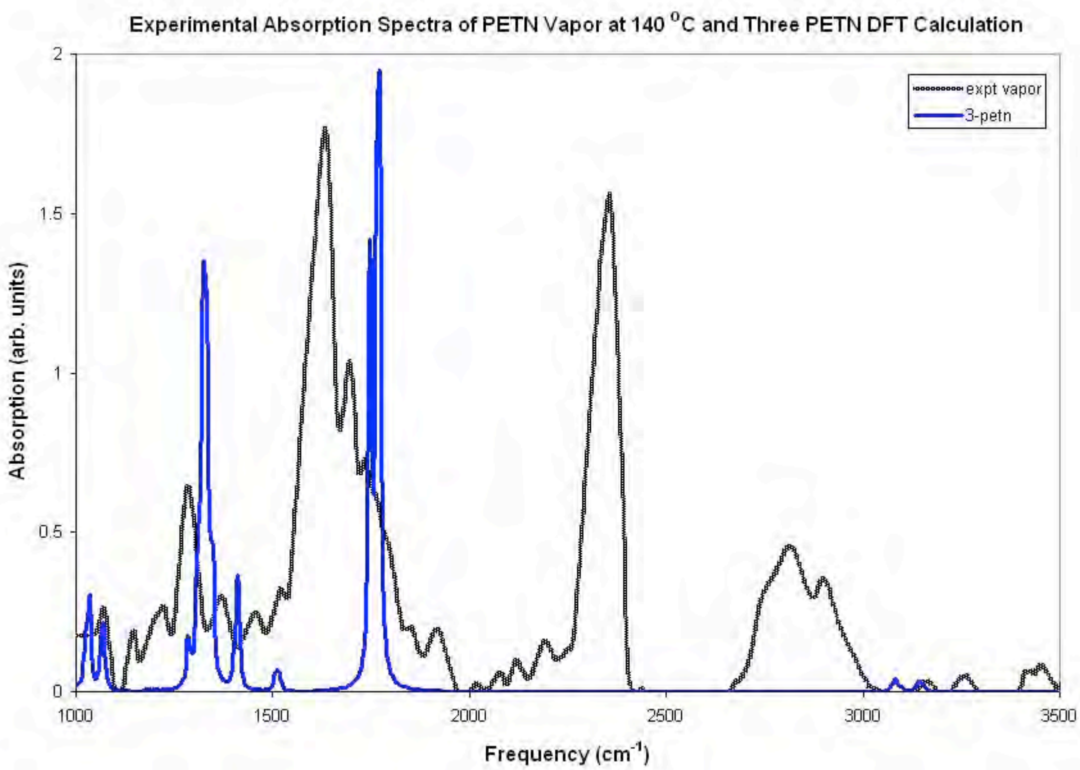


**Figure 19(b).** Qualitative comparison of DFT calculated spectra for three PETN and experimentally measured spectrum for dielectric response of PETN vapor.

**Table 11.** Comparison of DFT calculated and experimentally measured frequencies at prominent absorptions for PETN solid [19].

| Expt($cm^{-1}$) | 67 | 72 | 96 |
|---|---|---|---|
| 1-PETN | 56 | - | (125) |
| 3-PETN | 54-68 | 82 | (124) |

Referring to Figs. 19, one observes on average a noticeable correlation between DFT calculated spectra for molecule clusters of PETN and experimentally measured spectrum for dielectric response of PETN vapor. Shown in Table 12 is a comparison of DFT calculated frequencies corresponding to prominent absorptions, which have been observed experimentally for PETN in vapor state. Referring to this table, one can observe a high correlation between DFT calculated spectra for different cluster sizes and experimentally determined absorption lines at the specific frequencies indicated.

**Table 12.** Comparison of DFT calculated and experimentally measured frequencies at prominent absorptions for PETN vapor [20].

| Expt($cm^{-1}$) | 1279 | 1626 |
|---|---|---|
| 1-PETN | 1329 | 1768 |
| 3-PETN* | 1326 | 1746 |

## Ground State Resonance Structure of Molecular Clusters of TNT

In this section are presented the results of computational experiments using DFT concerning molecular clusters of TNT. These results include the relaxed or equilibrium configuration of a single isolated molecule of TNT (see Table 13) and ground-state oscillation frequencies and IR intensities for this configuration, which are calculated by DFT according to the frozen phonon approximation (see Table 14). The ground state resonance structure for a single isolated molecule of TNT is adopted as a reference for analysis of spectral features associated with molecular clusters of different sizes. For these calculations geometry optimization and vibrational analysis was effected using the DFT model B3LYP [12, 13] and basis function 6-311G(2d,2p) [14,15]. According to the specification of this basis function, (2d,2p) designates polarization functions having 2 sets of d functions for heavy atoms and 2 sets of p functions for hydrogen atoms [16]. A schematic representation of the molecular geometry of a single isolated molecule of TNT is shown in Fig. 20. A schematic representation of molecular geometries of molecular clusters consisting of 2 and 4 molecules are shown in Figs. 21 and 22, respectively. It is significant to note that the relative positions of the molecules associated with each of the molecular clusters is according to crystallographic structure conditions that would be associated with bulk material. In particular, the crystal structure of TNT, whose CCDC reference code is ZZZMUC05, has been investigated by N. I. Golovina, A. N. Raevskii, L. O. Atovmyan (1994) [22]. The space group for this crystal structure is ***P****21ab* (symmetry operators are x, y, z; x, ½+y, -z; ½+x, -y, -z; ½+x, ½-y, z), and the unit cell constants are a=20.041, b=15.013, c=6.084, $\alpha$=90.00, $\beta$=90.00, $\gamma$=90.00 and density 1.648 g/cm$^3$. The ground-state oscillation frequencies and IR intensities for the different molecular clusters of TNT, corresponding to their relaxed equilibrium configurations, are calculated by DFT according to the frozen phonon approximation. In the cases of molecular clusters of 2 and 4 molecules, these values are given in Tables 15 and 16, respectively. The DFT model and basis function used for these calculations are the same as those used for the single isolated molecule of TNT.

**Table 13.** Atomic positions for equilibrium configuration of TNT (Å)

| Atomic number | X | Y | Z | Atomic number | X | Y | Z |
|---|---|---|---|---|---|---|---|
| 1 | 1.294359 | -0.627693 | 1.916458 | 6 | 1.399735 | -0.432944 | -2.779328 |
| 1 | -2.458208 | -0.867791 | -0.128619 | 7 | -1.347001 | -0.883583 | 2.313715 |
| 1 | 0.754635 | 0.052629 | -3.504585 | 7 | 2.841751 | -0.500544 | -0.177322 |
| 1 | 1.68668 | -1.400164 | -3.189867 | 7 | -1.547799 | -0.781608 | -2.569596 |
| 1 | 2.304987 | 0.153675 | -2.659394 | 8 | 3.474661 | -1.155138 | -0.992685 |
| 6 | 0.730091 | -0.664364 | 0.998736 | 8 | 3.321537 | 0.203741 | 0.698298 |
| 6 | -0.646569 | -0.782893 | 1.016672 | 8 | -0.658543 | -0.86075 | 3.323182 |
| 6 | -1.382696 | -0.799534 | -0.152696 | 8 | -2.564711 | -0.982781 | 2.284321 |
| 6 | -0.701136 | -0.724375 | -1.355556 | 8 | -2.607727 | -0.174823 | -2.533999 |
| 6 | 0.693755 | -0.609698 | -1.463028 | 8 | -1.14092 | -1.451907 | -3.507164 |
| 6 | 1.364308 | -0.592195 | -0.229936 | | | | |

**Table 14.** Oscillation frequencies and IR intensities for single isolated molecule of TNT.

| Frequency $cm^{-1}$ | Intensity (km/mol) | Frequency $cm^{-1}$ | Intensity (km/mol) | Frequency $cm^{-1}$ | Intensity (km/mol) | Frequency $cm^{-1}$ | Intensity (km/mol) |
|---|---|---|---|---|---|---|---|
| 48.1344 | 0.1511 | 470.7113 | 1.3672 | 960.2885 | 2.6521 | 1479.3087 | 11.0602 |
| 54.4696 | 0.0031 | 481.9805 | 0.0293 | 966.588 | 10.2579 | 1495.7421 | 9.6734 |
| 54.6314 | 0.449 | 541.3526 | 1.0016 | 1046.3734 | 3.8264 | 1608.9564 | 75.6162 |
| 95.2736 | 4.9386 | 548.7636 | 2.1862 | 1051.7325 | 1.107 | 1626.0082 | 155.939 |
| 120.4472 | 4.6364 | 662.2958 | 9.245 | 1093.3557 | 53.251 | 1637.3636 | 7.7795 |
| 149.4345 | 2.5947 | 667.0623 | 0.0724 | 1183.9727 | 9.8852 | 1668.2966 | 226.3714 |
| 176.8858 | 0.2872 | 717.9113 | 20.7181 | 1208.2366 | 14.9414 | 1668.9285 | 185.4888 |
| 187.9397 | 0.1349 | 739.4252 | 51.7192 | 1220.3445 | 0.256 | 3075.5823 | 0.8369 |
| 195.623 | 4.7398 | 760.6036 | 27.3511 | 1354.5992 | 4.7978 | 3143.8171 | 5.2936 |
| 296.0832 | 1.9743 | 790.626 | 0.2088 | 1389.0625 | 326.8959 | 3175.73 | 4.0642 |
| 324.2345 | 0.2144 | 797.0792 | 6.7309 | 1392.5596 | 309.3893 | 3256.9297 | 12.3643 |
| 327.7225 | 0.0382 | 805.7737 | 11.3147 | 1402.1146 | 5.7057 | 3257.0266 | 29.788 |
| 352.9275 | 2.4697 | 843.4395 | 1.7202 | 1422.838 | 4.377 | | |
| 367.8506 | 1.3391 | 919.629 | 37.1859 | 1423.0629 | 6.7083 | | |
| 386.8114 | 1.1556 | 951.7191 | 31.8976 | 1475.6511 | 2.6229 | | |

**Table 15.** Oscillation frequencies and IR intensities for 2-molecule cluster of TNT.

| Frequency $cm^{-1}$ | Intensity (km/mol) | Frequency $cm^{-1}$ | Intensity (km/mol) | Frequency $cm^{-1}$ | Intensity (km/mol) | Frequency $cm^{-1}$ | Intensity (km/mol) |
|---|---|---|---|---|---|---|---|
| 8.1269 | 0.0355 | 352.9561 | 1.8829 | 843.0377 | 0.4042 | 1421.4177 | 9.6829 |
| 9.2439 | 0.1381 | 353.7762 | 2.7653 | 844.2998 | 3.981 | 1422.4552 | 5.9836 |
| 14.9722 | 0.1304 | 367.1677 | 1.2469 | 921.465 | 5.1014 | 1424.182 | 3.6857 |
| 17.9857 | 0.0806 | 368.4943 | 1.7859 | 922.0174 | 62.7738 | 1424.5634 | 7.0426 |
| 27.8664 | 0.1452 | 385.1874 | 1.5395 | 952.5892 | 34.8719 | 1475.9287 | 9.638 |
| 51.3591 | 0.1152 | 387.5417 | 1.2049 | 953.1544 | 30.8313 | 1476.429 | 0.6661 |
| 52.1877 | 0.1647 | 470.4774 | 0.6591 | 959.6472 | 4.1415 | 1477.5623 | 5.8383 |
| 54.9708 | 0.1831 | 471.4932 | 1.4576 | 960.2688 | 2.7507 | 1480.2882 | 9.2747 |
| 56.1668 | 0.0134 | 482.1479 | 0.0734 | 966.3623 | 10.1398 | 1499.3215 | 7.3228 |
| 59.7929 | 0.3965 | 483.016 | 0.4663 | 966.7785 | 10.4861 | 1501.9449 | 6.629 |
| 78.491 | 1.4342 | 541.2321 | 0.2644 | 1048.9553 | 3.3337 | 1607.2729 | 14.1997 |
| 89.0883 | 0.0858 | 541.4728 | 3.0752 | 1050.6176 | 4.1689 | 1608.0475 | 147.0028 |
| 101.2143 | 7.358 | 548.9486 | 0.5345 | 1052.5814 | 2.3397 | 1620.5898 | 76.0466 |
| 103.5822 | 5.1626 | 549.1266 | 5.0519 | 1056.3804 | 1.6056 | 1624.0647 | 230.3202 |
| 123.1052 | 6.1392 | 661.4668 | 18.0395 | 1094.1389 | 39.3235 | 1633.2048 | 22.9768 |
| 127.3796 | 3.0096 | 662.5497 | 2.1107 | 1094.3667 | 64.4747 | 1634.0034 | 18.3162 |
| 150.451 | 3.4095 | 668.0229 | 0.449 | 1184.6285 | 15.6223 | 1664.0026 | 50.159 |
| 153.1326 | 1.5344 | 668.7801 | 0.2078 | 1184.7833 | 4.4717 | 1667.4041 | 334.8076 |
| 179.5611 | 0.7559 | 717.8515 | 14.8535 | 1208.917 | 6.8039 | 1668.4406 | 210.3268 |
| 185.8249 | 1.666 | 718.1848 | 26.9107 | 1209.2321 | 26.3875 | 1669.2795 | 166.2294 |
| 189.4679 | 0.2125 | 739.2918 | 111.0234 | 1220.4561 | 0.3392 | 3074.9392 | 0.8768 |
| 193.7987 | 7.0708 | 740.0657 | 7.4066 | 1222.2325 | 0.3771 | 3075.6946 | 0.259 |
| 194.5187 | 1.3655 | 760.1704 | 33.4574 | 1354.3826 | 15.2785 | 3146.9888 | 2.6818 |
| 199.9836 | 2.5218 | 760.7635 | 22.866 | 1355.7351 | 7.5663 | 3147.3743 | 4.1554 |
| 296.0558 | 3.3548 | 790.55 | 0.2145 | 1388.4705 | 610.8024 | 3180.3569 | 1.1336 |
| 296.6949 | 0.8447 | 791.5138 | 0.1071 | 1389.1523 | 31.4292 | 3180.9182 | 3.7902 |
| 324.7901 | 0.2067 | 796.5846 | 2.8469 | 1392.7549 | 647.5478 | 3255.7366 | 23.6929 |
| 325.6773 | 0.2503 | 796.7956 | 10.0258 | 1394.4088 | 58.375 | 3257.2678 | 21.2765 |
| 326.5354 | 0.035 | 805.9091 | 21.8258 | 1402.6722 | 1.3532 | 3258.4272 | 17.8489 |
| 329.1659 | 0.2011 | 806.2351 | 2.4385 | 1405.172 | 40.3744 | 3260.5779 | 14.6354 |

**Table 16.** Oscillation frequencies and IR intensities for 4-molecule cluster of TNT.

| Frequency $cm^{-1}$ | Intensity (km/mol) | Frequency $cm^{-1}$ | Intensity (km/mol) | Frequency $cm^{-1}$ | Intensity (km/mol) | Frequency $cm^{-1}$ | Intensity (km/mol) |
|---|---|---|---|---|---|---|---|
| 6.0037 | 0.0276 | 190.2879 | 0.3889 | 659.3755 | 11.1961 | 962.0534 | 9.2311 |
| 6.8127 | 0.0135 | 192.0548 | 3.329 | 659.8872 | 3.4303 | 962.7248 | 8.0756 |
| 9.5511 | 0.0445 | 192.7032 | 0.5122 | 661.2794 | 13.0666 | 963.062 | 0.6791 |
| 10.7137 | 0.0363 | 196.8943 | 5.2073 | 662.7278 | 9.7932 | 966.6378 | 8.1237 |
| 13.1434 | 0.1926 | 198.2761 | 5.0334 | 667.572 | 0.5246 | 968.2356 | 9.3892 |
| 14.6485 | 0.0858 | 199.7631 | 0.4605 | 669.3944 | 0.0793 | 1043.2646 | 8.177 |
| 17.4745 | 0.0361 | 202.1056 | 5.8742 | 672.8601 | 4.6511 | 1044.2894 | 6.1182 |
| 19.1606 | 0.0969 | 294.9276 | 1.4559 | 673.2171 | 2.6274 | 1048.3198 | 5.3386 |
| 21.5413 | 0.0717 | 296.7783 | 1.0261 | 716.6365 | 24.5244 | 1050.1333 | 2.0496 |
| 25.5663 | 0.2335 | 297.8845 | 2.4338 | 716.9527 | 13.5797 | 1050.6147 | 3.5367 |
| 27.2907 | 0.0672 | 298.8831 | 4.4941 | 718.0088 | 22.1708 | 1050.6708 | 3.3637 |
| 28.3122 | 0.0329 | 324.7092 | 0.2389 | 719.3519 | 18.0592 | 1052.1492 | 5.8976 |
| 32.3861 | 0.1016 | 325.209 | 0.6029 | 739.063 | 24.7206 | 1052.735 | 4.1214 |
| 34.9573 | 0.2077 | 325.7378 | 0.148 | 739.3708 | 130.8296 | 1096.455 | 75.916 |
| 40.7299 | 0.3467 | 325.811 | 0.0405 | 739.7837 | 7.1419 | 1096.6624 | 54.0083 |
| 45.9148 | 0.5988 | 328.6621 | 0.7673 | 740.7033 | 70.2921 | 1097.9261 | 37.4622 |
| 50.9682 | 0.136 | 329.6841 | 0.4998 | 759.5333 | 23.6246 | 1100.058 | 41.0888 |
| 51.3221 | 0.1839 | 330.0564 | 0.8057 | 759.7645 | 42.8882 | 1185.3416 | 7.8041 |
| 51.9382 | 0.6017 | 332.9135 | 0.1063 | 761.1715 | 20.4302 | 1185.6052 | 16.1508 |
| 52.3798 | 0.3453 | 353.4549 | 2.2863 | 761.3542 | 30.9627 | 1185.7306 | 10.7674 |
| 54.6865 | 0.0232 | 353.8611 | 2.0427 | 790.5221 | 0.8358 | 1186.6664 | 12.6373 |
| 55.5157 | 0.0207 | 354.4024 | 2.9248 | 790.5998 | 0.8792 | 1209.8322 | 15.0783 |
| 57.1434 | 0.358 | 355.4821 | 3.7328 | 791.1676 | 2.192 | 1212.8856 | 15.3057 |
| 62.0863 | 1.2134 | 366.9194 | 1.0839 | 791.3026 | 0.1507 | 1214.3346 | 13.1397 |
| 67.9725 | 0.2731 | 368.2383 | 1.9205 | 795.9496 | 5.5813 | 1217.5505 | 16.2261 |
| 73.8181 | 1.3738 | 369.3088 | 3.9455 | 796.7322 | 4.9704 | 1219.2219 | 0.5039 |
| 82.7084 | 0.6903 | 371.3992 | 4.807 | 797.4355 | 0.6989 | 1222.7281 | 10.706 |
| 91.401 | 0.4921 | 384.9266 | 1.092 | 797.6327 | 9.7116 | 1222.955 | 1.1508 |
| 95.9635 | 1.9103 | 385.0972 | 1.1167 | 805.0269 | 12.7807 | 1223.564 | 1.0288 |
| 99.4256 | 0.6227 | 388.1738 | 0.4284 | 805.3314 | 9.2942 | 1351.2896 | 9.5548 |
| 102.8424 | 1.2621 | 391.668 | 1.9364 | 806.0565 | 12.7468 | 1353.3455 | 4.2628 |
| 103.8391 | 9.4549 | 463.06 | 0.3618 | 807.2446 | 17.6478 | 1354.8254 | 5.0704 |
| 110.2973 | 5.5524 | 467.1603 | 1.1573 | 842.8611 | 0.756 | 1355.7509 | 6.9006 |
| 112.2823 | 14.0066 | 471.2585 | 0.2994 | 843.3628 | 3.0391 | 1387.3927 | 504.0168 |
| 124.5235 | 5.1683 | 472.1674 | 1.6982 | 844.5015 | 1.8451 | 1388.4775 | 243.7943 |
| 130.0222 | 1.9675 | 481.0948 | 0.1812 | 845.4727 | 2.1841 | 1388.7524 | 87.4017 |
| 132.8818 | 2.7792 | 483.7679 | 0.597 | 921.0493 | 17.8875 | 1389.0958 | 447.19 |
| 135.3963 | 1.4377 | 484.3633 | 1.0706 | 922.0851 | 40.7448 | 1392.4327 | 798.6592 |
| 147.6898 | 2.1166 | 485.0125 | 0.3554 | 923.0247 | 45.2336 | 1393.287 | 243.6454 |
| 152.6375 | 5.3 | 540.766 | 2.8936 | 923.3955 | 28.3322 | 1394.8691 | 156.6218 |
| 153.1419 | 2.6393 | 541.2985 | 1.5216 | 951.4396 | 6.7371 | 1396.2841 | 238.8504 |
| 157.2293 | 1.2297 | 542.3571 | 0.716 | 951.9678 | 39.1078 | 1402.8853 | 40.1082 |
| 165.0722 | 0.1527 | 542.7461 | 2.9325 | 953.4363 | 32.0243 | 1405.0447 | 2.3998 |
| 175.0778 | 0.79 | 549.0063 | 3.0966 | 953.5462 | 24.8804 | 1405.257 | 35.9898 |
| 178.4232 | 1.1197 | 549.4428 | 5.5645 | 954.3428 | 34.9316 | 1408.3396 | 49.7168 |
| 184.5245 | 1.3816 | 550.4266 | 3.418 | 955.4679 | 4.9786 | 1419.1819 | 11.4361 |
| 188.0139 | 2.7537 | 551.0865 | 2.0792 | 960.9208 | 3.5001 | 1419.2982 | 4.5842 |

**Table 16 (continued)**

| Frequency cm$^{-1}$ | Intensity (km/mol) | Frequency cm$^{-1}$ | Intensity (km/mol) | Frequency cm$^{-1}$ | Intensity (km/mol) | Frequency cm$^{-1}$ | Intensity (km/mol) |
|---|---|---|---|---|---|---|---|
| 1420.2479 | 5.2822 | 1497.4508 | 11.3855 | 1659.2784 | 20.6782 | 3152.1172 | 3.5304 |
| 1420.9575 | 11.7015 | 1499.9305 | 5.7411 | 1660.0342 | 35.6986 | 3177.7893 | 3.8554 |
| 1424.3171 | 6.9025 | 1499.9749 | 6.4007 | 1663.2992 | 146.911 | 3182.9602 | 2.5709 |
| 1424.7 | 14.2952 | 1602.7976 | 89.5147 | 1664.3833 | 383.5529 | 3190.4402 | 3.017 |
| 1425.6173 | 3.7006 | 1604.576 | 75.0732 | 1666.8501 | 298.8433 | 3204.1228 | 1.4827 |
| 1426.0646 | 3.5978 | 1605.7961 | 16.9799 | 1668.7557 | 154.036 | 3231.541 | 99.6425 |
| 1473.5498 | 9.0424 | 1606.5385 | 136.8389 | 1669.1105 | 13.3956 | 3253.373 | 20.5025 |
| 1474.6635 | 12.8272 | 1614.0665 | 33.3701 | 1669.4171 | 381.2602 | 3255.3308 | 23.642 |
| 1475.9045 | 16.0343 | 1615.7209 | 24.6628 | 3073.4512 | 2.0504 | 3255.5933 | 23.5913 |
| 1476.1462 | 5.7658 | 1617.3809 | 316.2843 | 3075.5383 | 0.5901 | 3256.0857 | 22.1997 |
| 1476.3361 | 10.2827 | 1623.7596 | 58.5519 | 3076.5342 | 0.1196 | 3257.0527 | 24.6223 |
| 1477.5513 | 3.2443 | 1624.993 | 121.0073 | 3076.7654 | 0.9591 | 3258.084 | 18.7786 |
| 1477.8824 | 21.6264 | 1630.8451 | 12.1011 | 3143.1304 | 3.4185 | 3265.4907 | 18.7129 |
| 1478.4861 | 10.8031 | 1632.7219 | 102.004 | 3149.0393 | 8.8789 | | |
| 1494.5078 | 2.0778 | 1634.2406 | 2.0151 | 3149.7698 | 4.0967 | | |

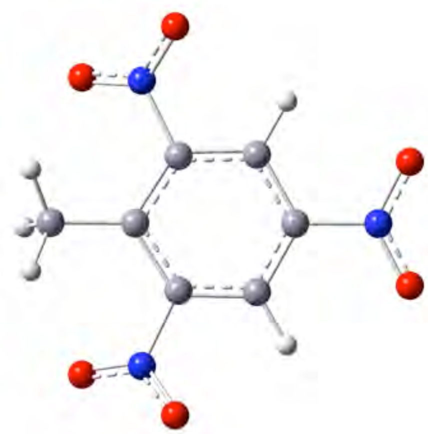

**Figure 20.** Molecular geometry of TNT

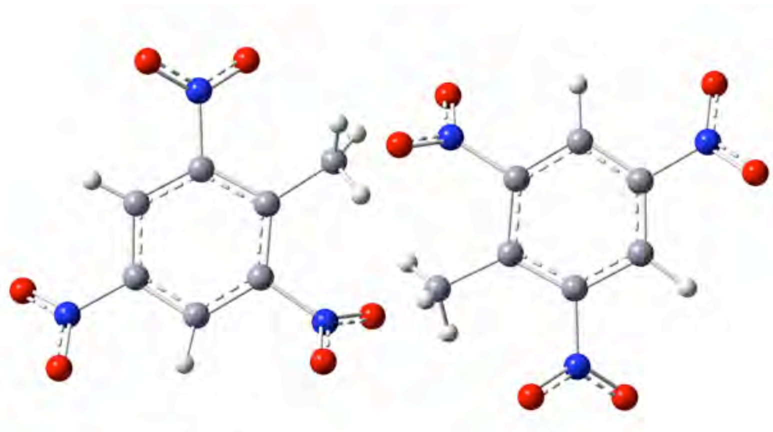

**Figure 21.** Molecular geometry of 2-molecule cluster of TNT

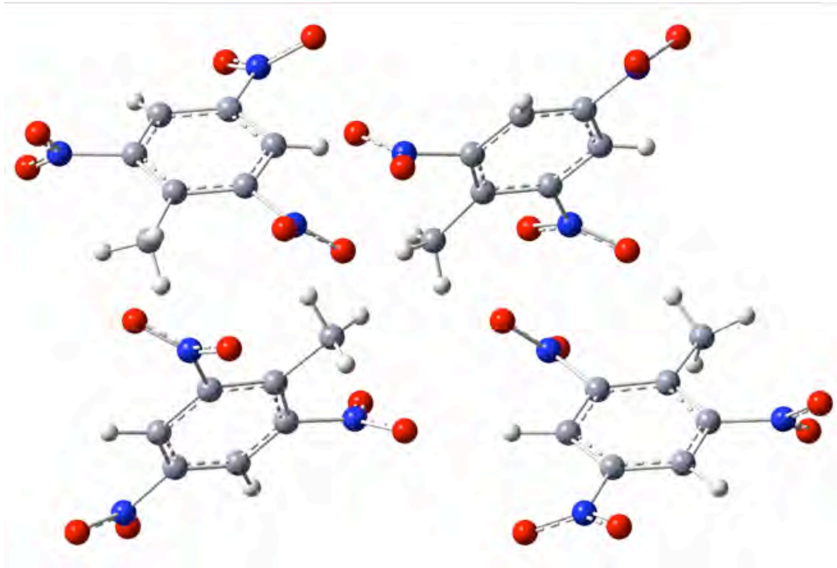

**Figure 22.** Molecular geometry of 4-molecule cluster of TNT

Proceeding, shown in Figs. 23, 24 and 25 are calculated IR intensities for a single isolated molecule and molecular clusters consisting of 2 and 4 molecules of TNT, respectively. Shown in Figs. 26, 27 and 28, are continuous spectra consisting of a superposition of essentially Lorenzian functions of various heights and widths, which have been constructed using the discrete spectra given in Tables 14, 15 and 16, respectively.

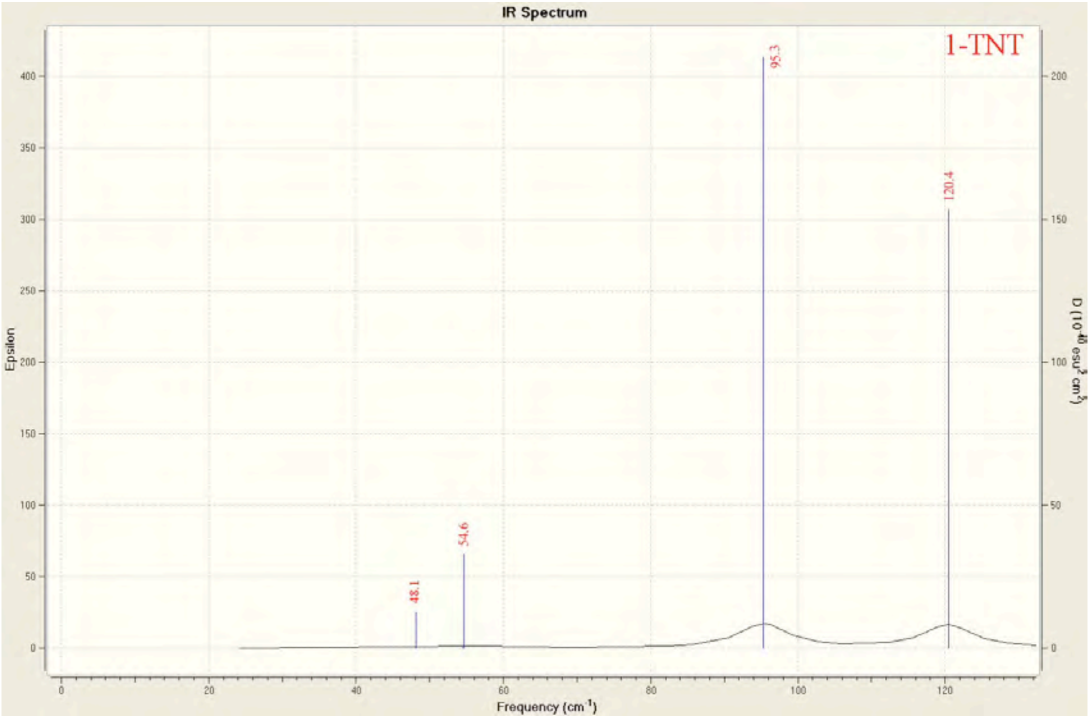


**Figure 23.** IR intensity as a function of frequency calculated using DFT B3LYP/6-311G(2d,2p) for single isolated molecule of TNT according to frozen phonon approximation.

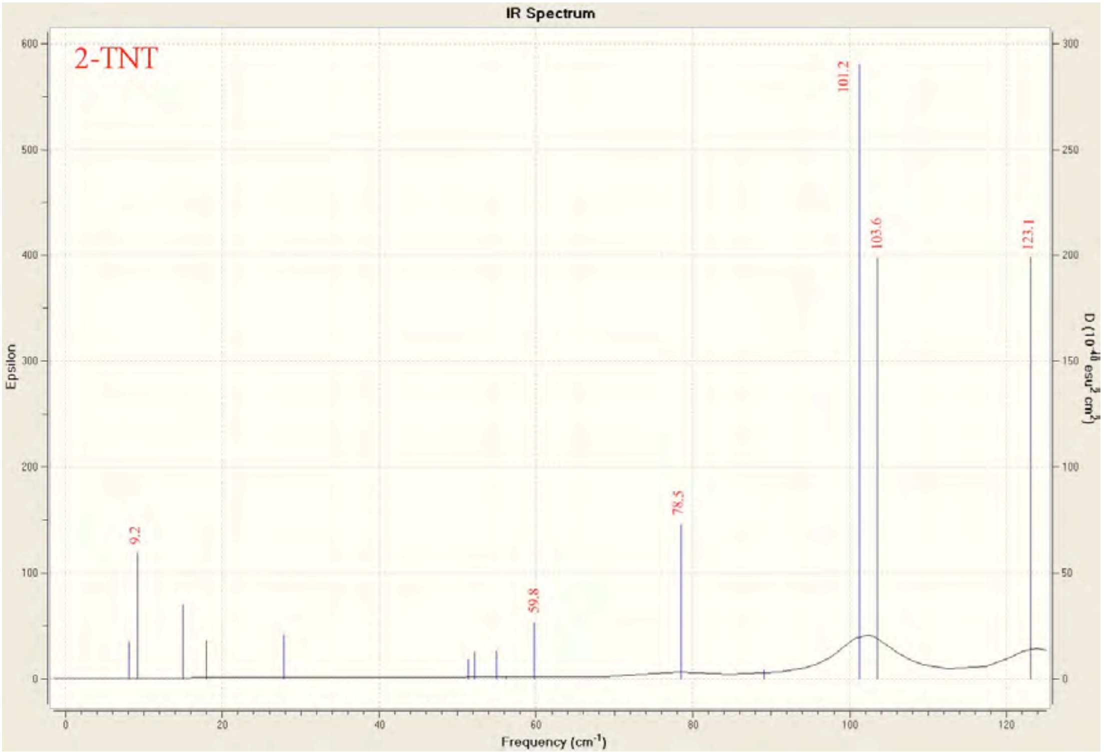


**Figure 24.** IR intensity as a function of frequency calculated using DFT B3LYP/6-311G(2d,2p) for two-molecule cluster of TNT according to frozen phonon approximation.

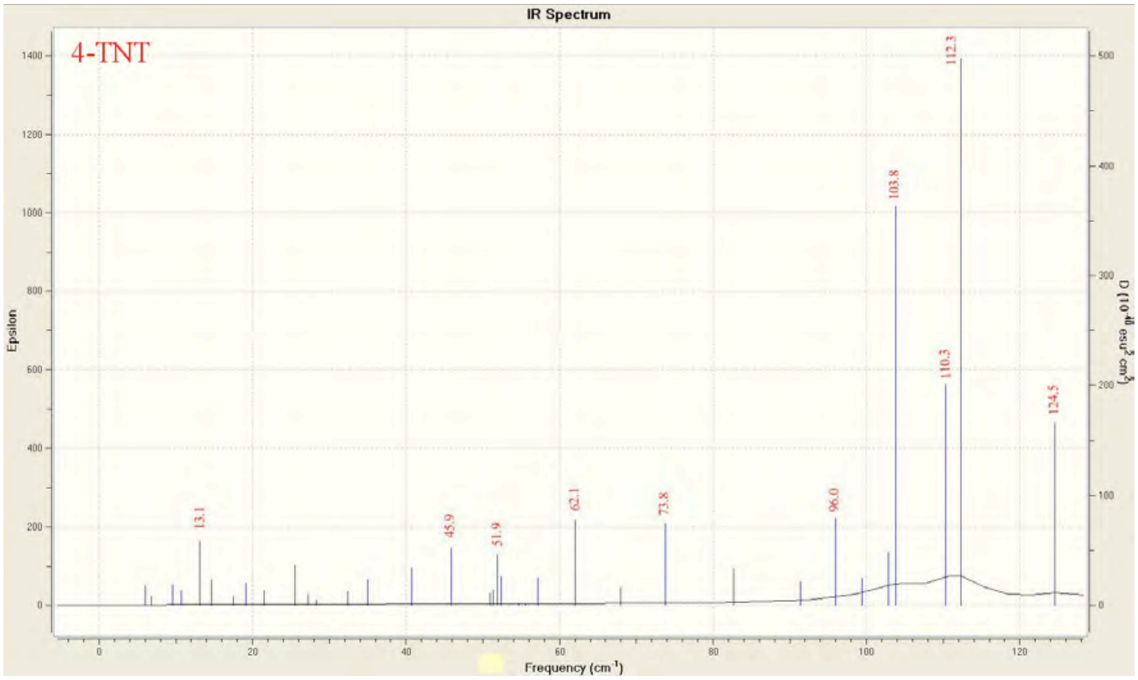


**Figure 25.** IR intensity as a function of frequency calculated using DFT B3LYP/6-311G(2d,2p) for four-molecule cluster of TNT according to frozen phonon approximation.

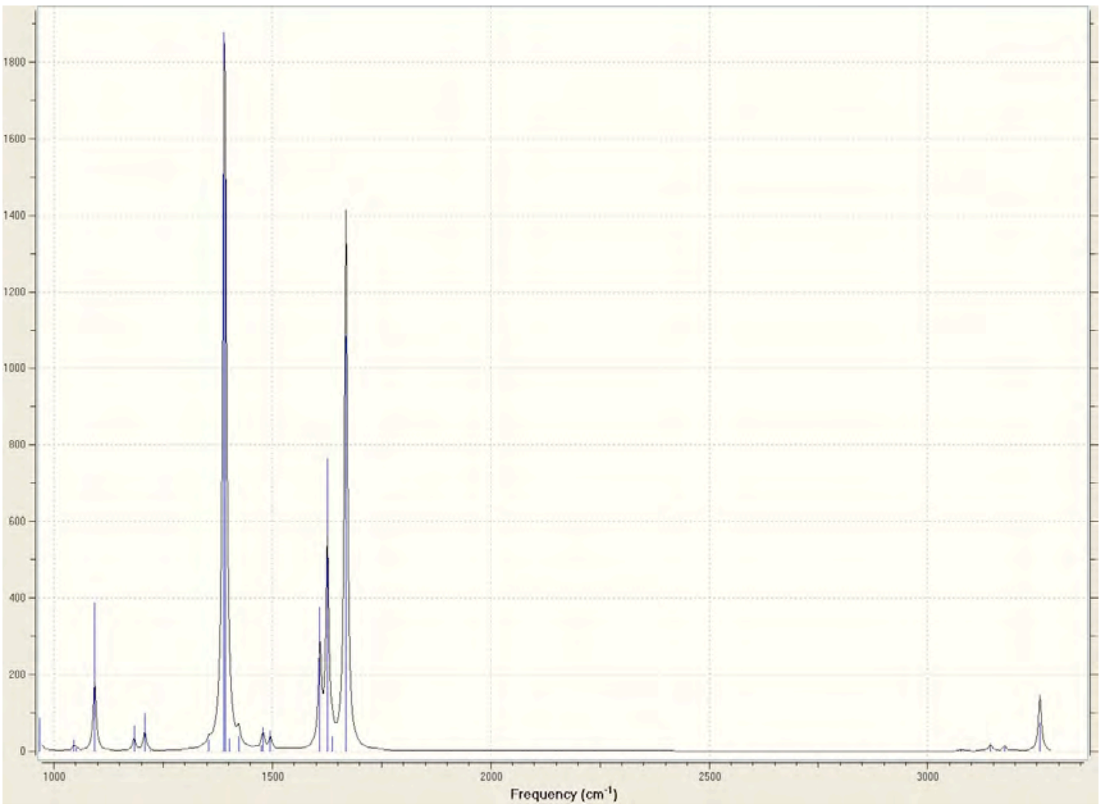


**Figure 26.** Continuous-spectrum representation of IR intensity as a function of frequency calculated using DFT for single isolated molecule of TNT.

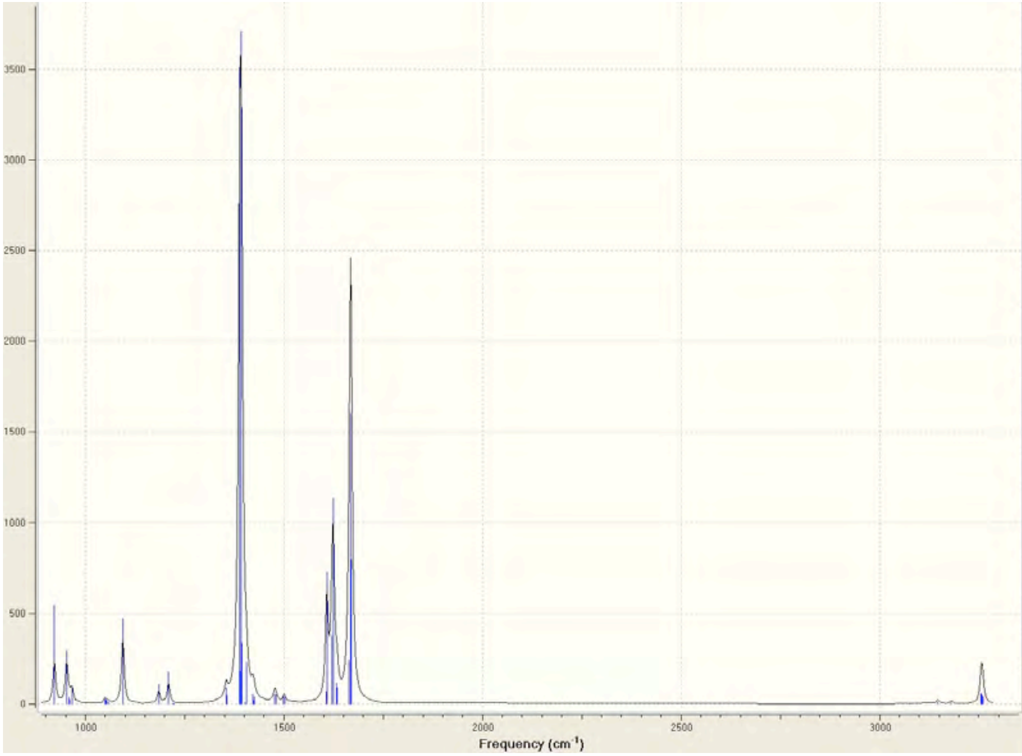

**Figure 27.** Continuous-spectrum representation of IR intensity as a function of frequency calculated using DFT for two-molecule cluster of TNT.

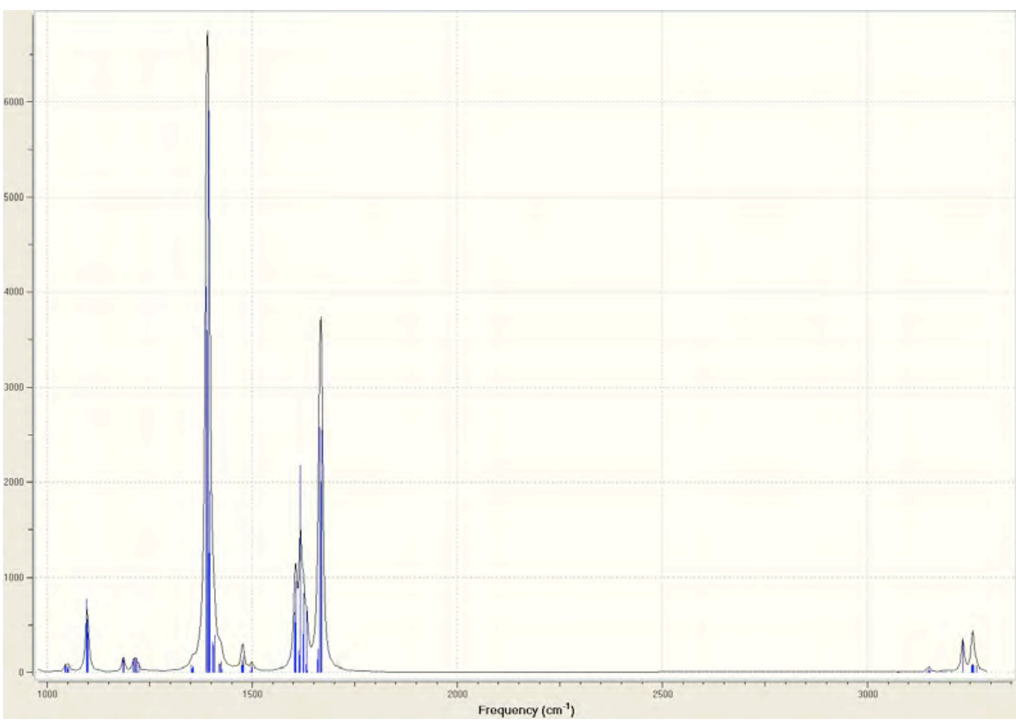

**Figure 28.** Continuous-spectrum representation of IR intensity as a function of frequency calculated using DFT for two-molecule cluster of TNT.

Shown in Figs. 29 and 30 are spectra of clusters in comparison with experimentally measured spectra [19, 20]. Referring to these figures, initial consideration is given to what extent various average features of the DFT calculated spectra for different size molecular clusters, as well as experimentally measured spectra, are correlated with each other. Referring to Fig. 29, one observes on average a noticeable correlation between DFT calculated spectra for molecule clusters of TNT and experimentally measured spectrum for dielectric response of TNT solid. The comparison of spectra shown in Fig. 29 also supports the notion that certain resonance features, which are associated with finite-size molecular clusters, are preserved within clusters of increasing size, as well as in solid form, thus implying a persistence of these modes after coupling to intermolecular influences. The persistence of certain intramolecular modes, which is irrespective of molecular cluster size, i.e., whether the molecule is isolated, part of a cluster or within a bulk lattice, is demonstrated by comparison of DFT calculated and experimentally measured spectra. Shown in Table 17 is a comparison of DFT calculated frequencies corresponding to prominent absorptions, which have been observed experimentally for TNT in solid state. Referring to this table, one can observe a high correlation between DFT calculated spectra for different cluster sizes and experimentally determined absorption lines at the specific frequencies indicated.

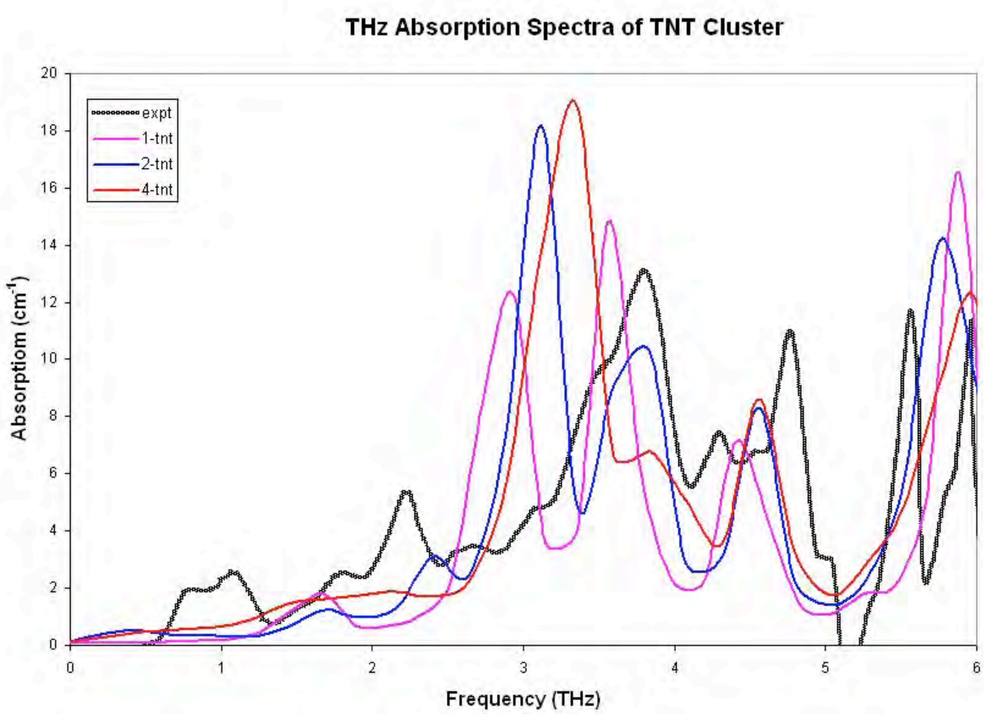


Figure 29. Qualitative comparison of DFT calculated spectra for 1-and 3-molecule clusters of TNT and experimentally measured spectrum for dielectric response of TNT solid.

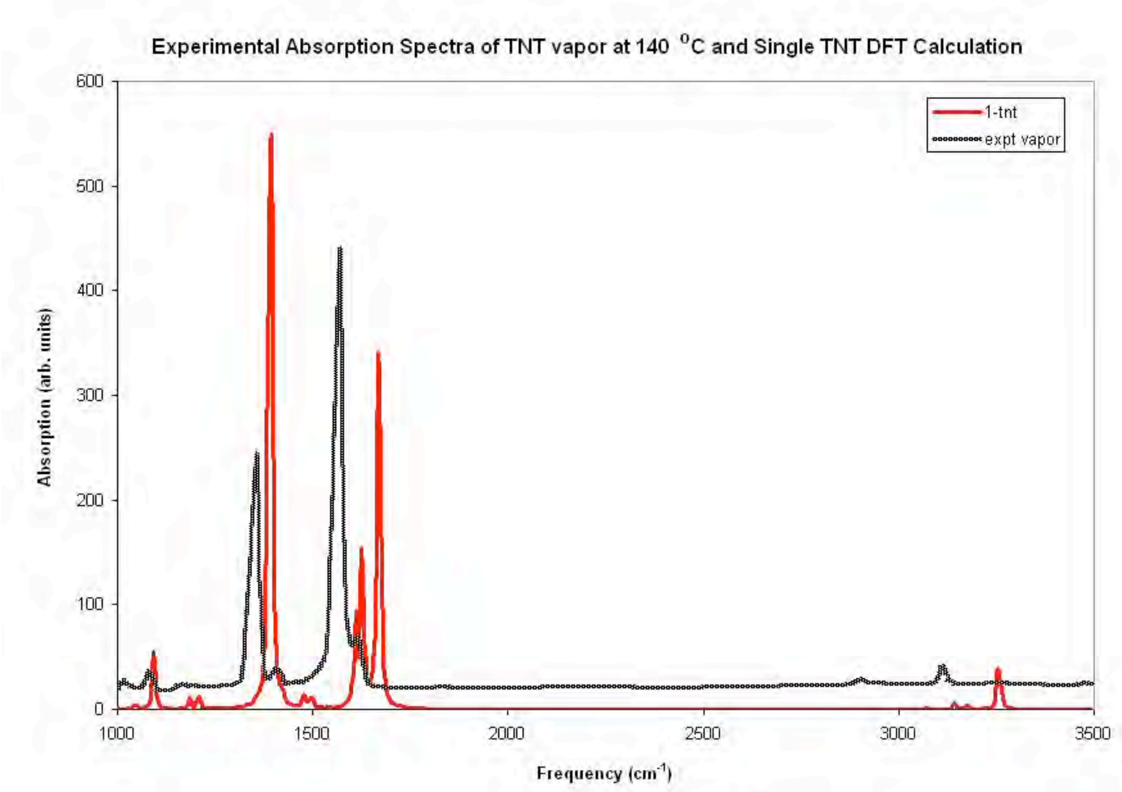


Figure 30(a). Qualitative comparison of DFT calculated spectra for single TNT and experimentally measured spectrum for dielectric response of TNT vapor.

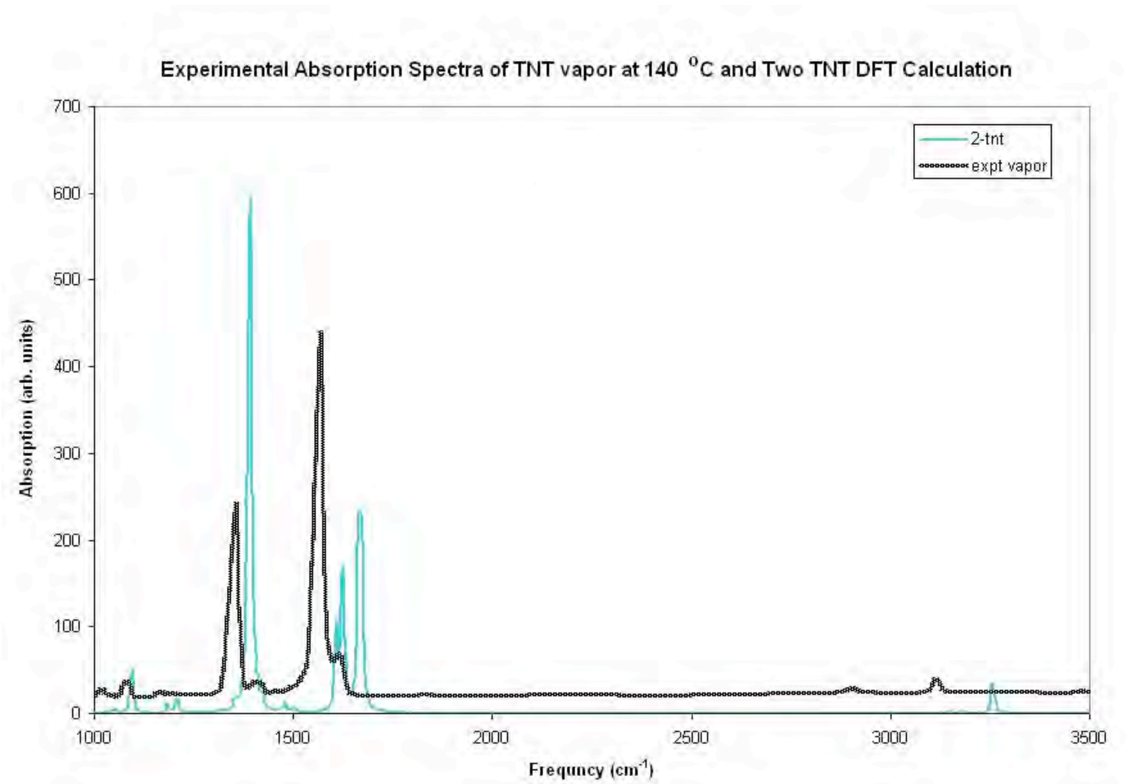


Figure 30(b). Qualitative comparison of DFT calculated spectra for 2-molecule clusters of TNT and experimentally measured spectrum for dielectric response of TNT vapor.

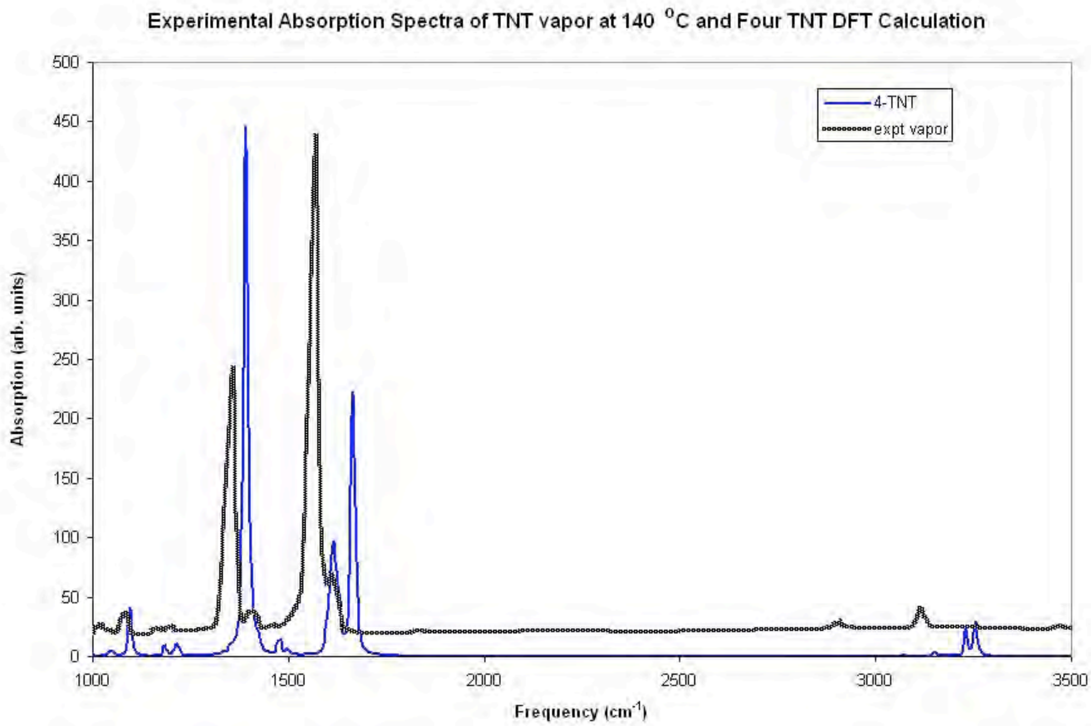


Figure 30(c). Qualitative comparison of DFT calculated spectra for 4-molecule clusters of TNT and experimentally measured spectrum for dielectric response of TNT vapor.

**Table 17.** Comparison of DFT calculated and experimentally measured frequencies at prominent absorptions for TNT solid [19].

| Expt($cm^{-1}$) | 53 | 73 | | 127 |
|---|---|---|---|---|
| 1-TNT | 48-55 | (95) | | 120 |
| 2-TNT | 60 | 79 | (101-103) | 123 |
| 4-TNT | 52 | 74 | (104-112) | 125 |

Referring to Fig. 30, one observes on average a noticeable correlation between DFT calculated spectra for molecule clusters of TNT and experimentally measured spectrum for dielectric response of TNT vapor. Shown in Table 18 is a comparison of DFT calculated frequencies corresponding to prominent absorptions, which have been observed experimentally for TNT in vapor state. Referring to this table, one can observe a high correlation between DFT calculated spectra for different cluster sizes and experimentally determined absorption lines at the specific frequencies indicated.

**Table 18.** Comparison of DFT calculated and experimentally measured frequencies at prominent absorptions for TNT vapor [20].

| Expt($cm^{-1}$) | 1080 | 1349 | 1402 | 1559 | 1606 | 2898 | 3107 |
|---|---|---|---|---|---|---|---|
| Paper calc. | | 1651 | | 1880 | | 3244 | 3440 |
| | | 1654 | | 1883 | | 3324 | 3441 |
| | | | | | | 3348 | |
| 1-TNT | 1093 | 1389 | 1392 | 1479-95 | 1608-68 | 3143 | 3257 |
| 2-TNT* | 1094 | 1388 | 1393 | 1480-99 | 1608-67 | 3146 | 3255 |
| 4-TNT* | 1096 | 1387 | 1392 | 1477 | 1617-69 | 3149 | 3231 |

## Conclusion

The calculations of ground state resonance structure associated with molecular clusters of RDX, PETN and TNT using DFT are meant to serve as reasonable estimates of molecular level response characteristics, providing interpretation of dielectric response features, for subsequent adjustment relative to experimental measurements and molecular structure theory.

## Acknowledgement

This work was supported by the Office of Naval Research.

## References


[1] M. J. Frisch, G. W. Trucks, H. B. Schlegel, G. E. Scuseria, M. A. Robb, J. R. Cheeseman, G. Scalmani, V. Barone, B. Mennucci, G. A. Petersson, H. Nakatsuji, M. Caricato, X. Li, H. P. Hratchian, A. F. Izmaylov, J. Bloino, G. Zheng, J. L. Sonnenberg, M. Hada, M. Ehara, K. Toyota, R. Fukuda, J. Hasegawa, M. Ishida, T. Nakajima, Y. Honda, O. Kitao, H. Nakai, T. Vreven, J. A. Montgomery, Jr., J. E. Peralta, F. Ogliaro, M. Bearpark, J. J. Heyd, E. Brothers, K. N. Kudin, V. N. Staroverov, R. Kobayashi, J. Normand, K. Raghavachari, A. Rendell, J. C. Burant, S. S. Iyengar, J. Tomasi, M. Cossi, N. Rega, J. M. Millam, M. Klene, J. E. Knox, J. B. Cross, V. Bakken, C. Adamo, J. Jaramillo, R. Gomperts, R. E. Stratmann, O. Yazyev, A. J. Austin, R. Cammi, C. Pomelli, J. W. Ochterski, R. L. Martin, K. Morokuma, V. G. Zakrzewski, G. A. Voth, P. Salvador, J. J. Dannenberg, S. Dapprich, A. D. Daniels, Ö. Farkas, J. B. Foresman, J. V. Ortiz, J. Cioslowski, and D. J. Fox, Gaussian 09, Revision A.1, Gaussian, Inc., Wallingford CT, 2009.

[2] A. Frisch, M. J. Frisch, F. R. Clemente and G. W. Trucks, Gaussian 09 User's Reference, pp105-106 (2009)

[3] P. Hohenberg and W. Kohn, "Inhomogeneous Electron Gas" Phys. Rev. **136**, B864, (1964).

[4] W. Kohn and L. J. Sham, "Self-Consistent Equations Including Exchange and Correlation Effects" Phys. Rev. **140**, A1133 (1965).

[5] R.O. Jones and O. Gunnarson, "The density functional formalism, its applications and prospects" Rev. Mod. Phys. **61**, 689 (1989).

[6] W.W. Hager and H. Zhang, "A survey of nonlinear conjugate gradient methods," Pacific J. Optim., 2, p. 35-58 (2006).

[7] R. M. Martin, *Electronic Structures Basic Theory and Practical Methods*, Cambridge University Press, Cambridge 2004, p. 25.

[8] E. B. Wilson, J. C. Decius and P. C. Cross, *Molecular Vibrations* (McGraw-Hill, New York, 1955).

[9] J.W. Ochterski, "Vibrational Analysis in Gaussian," help@gaussian.com, 1999.

[10] C. A. D. Roeser and E. Mazur, "Light-Matter Interactions on Femtosecond Time Scale" in *Frontiers of Optical Spectroscopy*, eds. B. Di Bartolo and O. Forte, NATO Science Series v. 168 p. 29, Kluwer Academic Publishers, Dordrecht – Norwell, 2005; C. F. Bohren and D. R. Huffman, *Absorption and Scattering of Light by Small Particles* (Wiley-VCH Verlag, Weinheim, 2004).

[11] A. Shabaev, S. G. Lambrakos, N. Bernstein, V. L. Jacobs, D. Finkenstadt, "A General Framework for Numerical Simulation of IED-Detection Scenarios using Density Functional Theory and THz Spectra," Applied Spectroscopy, **65**, 409-416 (2011).

[12] A. D. Becke, "Density-functional Thermochemistry. III. The Role of Exact Exchange", *J. Chem. Phys.* **98**, 5648-5652 (1993).

[13] B. Miehlich, A. Savin, H. Stoll and H. Preuss, "Results of Obtained with the Correlation Energy Density Functionals of Becke and Lee, Yang and Parr", Chem. *Phys. Lett.* **157**, 200-206 (1989).

[14] A. D. McLean and G. S. Chandler, "Contracted Gaussian-basis sets for molecular calculations. 1. 2nd row atoms, Z=11-18," *J. Chem. Phys.*, **72** 5639-48 (1980).

[15] T. Clark, J. Chandrasekhar, G. W. Spitznagel and P. V. R. Schleyer, "Efficient diffuse function-augmented basis-sets for anion calculations. 3. The 3-21+G basis set for 1st-row elements, Li-F," *J. Comp. Chem.*, **4** 294-301, (1983).

[16] M. J. Frisch, J. A. Pople and J. S. Binkley, "Self-Consistent Molecular Orbital Methods. 25. Supplementary Functions for Gaussian Basis Sets," *J. Chem. Phys.*, **80** (1984) 3265-69.

[17] C.S. Choi and E. Prince, *Acta Crystallogr., Sect.B:Struct. Crystallogr.Cryst.Chem.* **28,** 2857-2862.

[18] I. J. Bruno, J. C. Cole, P. R. Edgington, M. K. Kessler, C. F. Macrae, P.McCabe, J. Pearson and R. Taylor, "*New software for seaching the Cambridge Structural Database and visualizing crystal structures*", Acta Cryst. (2002) B58, 389-397.

[19] T. Lo, I.S. Gregory, C. Baker, P.F. Taday, W.R. Tribe and M.C. Kemp, "The very far-infrared spectra of energetic materials and possible confusion materials using terahertz pulsed spectroscopy" *Vibrational Spectroscopy* 42 (2006) pp243-248.

[20] J. Janni, B.D. Gilbert, R.W. Field, and J.I. Steinfeld, "Infrared aborption of explosive molecule vapors" *Spectrochimica Acta* pat A 53 (1997) pp1375-1381.